INL/EXT-21-63346

High-Temperature Irradiation-Resistant Thermocouple Qualification Test Results Report

September 2021

Richard Skifton
Richard.Skifton@inl.gov

Idaho National Laboratory

INL is a U.S. Department of Energy National Laboratory
operated by Batelle Energy Alliance, LLC

INL/EXT-21-63346

High-Temperature Irradiation-Resistant Thermocouple Qualification Test Results Report

Richard Skifton
Richard.Skifton@inl.gov

September 2021

Idaho National Laboratory
Measurement Science Laboratory
Idaho Falls, Idaho 83401

http://www.inl.gov

Prepared for the
U.S. Department of Energy
Office of Nuclear Energy
Under DOE Idaho Operations Office
Contract DE-AC07-05ID14517

Page intentionally left blank

SUMMARY

This is a qualification report for the high-temperature irradiation-resistant thermocouple (HTIR-TC) developed by Nuclear Energy Enabling Technologies Advanced Sensors and Instrumentation program. Utilizing the Advanced Gas Reactor (AGR) 5/6/7 test conducted in the Advanced Test Reactor (ATR) at Idaho National Laboratory, the HTIR-TCs measured temperatures upwards of 1500°C during accident conditions. The HTIR-TCs are thus qualified to perform and withstand an 18-month refueling cycle typical of nuclear power plants at the normal operating temperature, with a drift of less than ±1%. The HTIR-TC is also qualified for incorporating into a test fixture during new fuels tests.

Page intentionally left blank

CONTENTS

FIGURES

TABLES

Page intentionally left blank

ACRONYMS

AGR	Advanced Gas Reactor
ATR	Advanced Test Reactor
BWR	Boiling-Water Reactor
EFPD	Effective Full-Power Days
EMF	Electromotive Force
EOL	End-of-Life
F&OR	Function and Operational Requirements
HTIR-TC	High-Temperature Irradiation-Resistant Thermocouple
PWR	Pressurized-Water Reactor
TC	Thermocouple

Page intentionally left blank

High-Temperature Irradiation-Resistant Thermocouple Qualification Test Results Report

1. GENERAL

High-temperature irradiation-resistant thermocouple (HTIR-TC) development has successfully passed through the design and calibration phase and entered the qualification phase. For the qualification test, the HTIR-TC underwent in-reactor testing for over 12 months in the Advanced Test Reactor (ATR)'s high-neutron-flux (perturbed thermal flux of up to ~ 2.8×10^{14} nv and fast flux of up to ~2.25×10^{14} nv), high-temperature (up to 1550°C) environment as part of the Advanced Gas Reactor (AGR) 5/6/7 fuel test. In this test, several HTIR-TCs were placed at various locations in the test fixture that was designed to evaluate the performance of new advanced fuel designs for the AGR program. This report provides the performance results of the HTIR-TCs in this reactor qualification test, and covers HTIR-TC performance features such as measurement range, accuracy, repeatability, drift, and end-of-life (EOL). It also describes how HTIR-TC performance meets the requirements listed in the HTIR-TC Qualification Test Requirement Report [1].

2. EXPERIMENTAL SETUP

Comprised of five (5) capsules, the AGR-5/6/7 fuel test fixture was located in the ATR reactor's northeast flux trap [2]. Figure 1 shows the capsules positioned in consecutive order, with Capsule 1 located at the furthest downward elevation, and Capsule 5 at the highest. The capsules contained varying amounts of test fuel that, in interacting with the ATR's neutron flux, produced temperatures that were measured by the thermocouples (TCs) in the capsules. This generated the required test data regarding fuel performance and, in turn, TC performance. The ATR's thermal neutron flux follows a symmetrical, cosine-squared profile, with maximum perturbed thermal flux values at the reactor height midplane at ~2.8×10^{14} nv, and a fast flux (E > 1 MeV) of approximately 2.25×10^{14} nv. The temperature range of each capsule varied due to placement in the reactor, and the temperature at each HTIR-TC varied depending on its location within the capsule. Capsule 3 was expected to show the highest temperatures, as it was placed at the reactor height midplane. One of the HTIR-TCs (i.e., 3-5) was located in the center of Capsule 3 and measured the highest sustained nuclear core temperature.

Construction and calibration of the HTIR-TCs used in the AGR-5/6/7 test followed the guidelines of the preliminary build and calibration reports, as well as specific controlled documents for each build [3, 4] and [5]. Furthermore, this report aligns with the performance requirements based on the function and operation requirements (F&OR) report [6].

Of the five capsules, only Capsules 1 and 3 contained installed HTIR-TCs to measure experimental temperatures. However, the lead wires for each TC must exit the reactor core by passing through designated channels in the upper capsules. This means, for instance, that the HTIR-TCs positioned for temperature measurement in Capsule 1 must pass through the high-thermal-neutron flux regions of the reactor core reflected in Capsule 3 (i.e., reactor height midplane). Thus, although the HTIR-TCs in Capsule 1 measure a lower temperature (as expected), the drift due to thermal- and fast-neutron-flux-induced changes of the cable thermoelements would be similar throughout all the TCs in Capsules 1 and 3.

The test fixture also had provision to pass a small, adjustable He-Ne mixture gas flow around the TCs to maintain a constant temperature and minimize the effect of power fluctuations on the TC temperature readings [7]. The gas flow was kept at a minimal value and did not remove heat by convection. The gas flow merely provided a high thermal conduction path to the cooler high-water flow of the reactor coolant outside the capsule housing serving as a heat sink for the capsules.

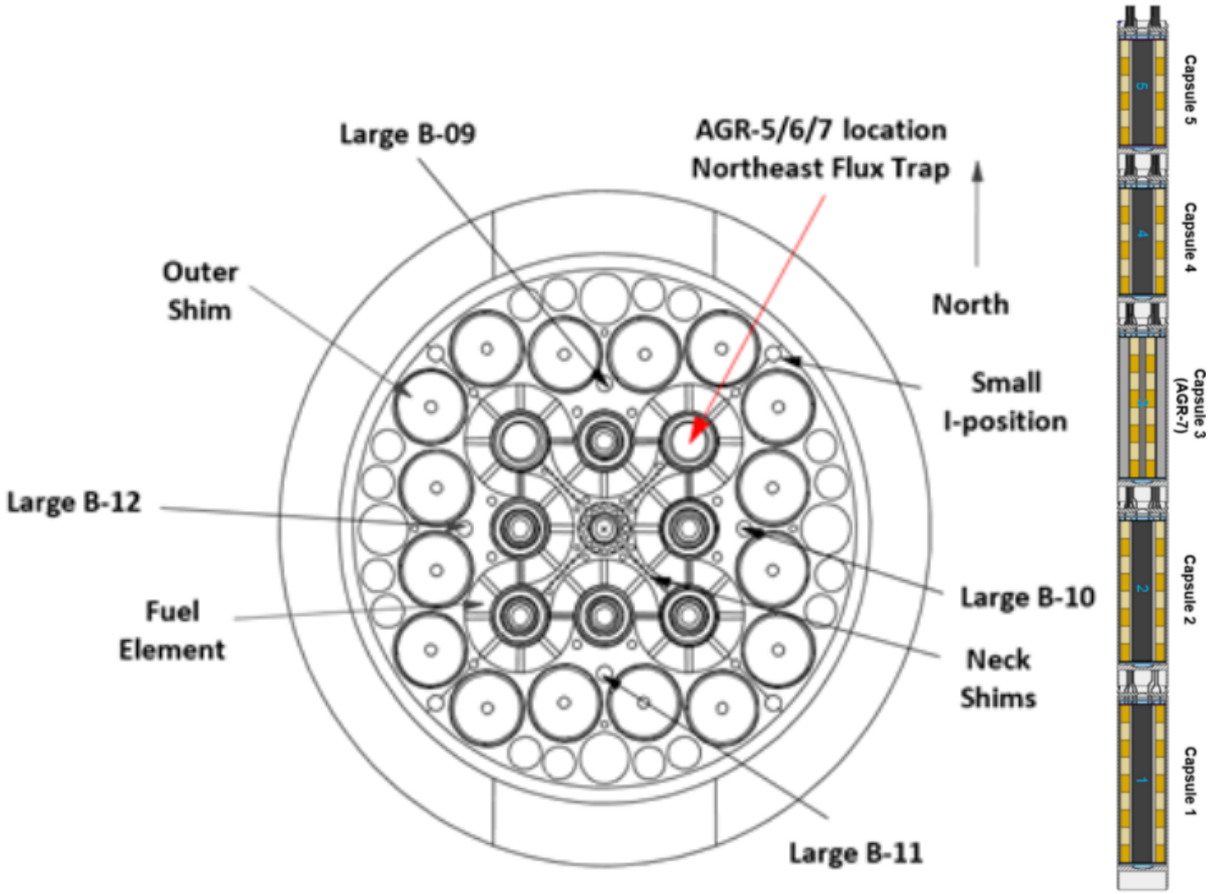

Figure 1. Layout of the AGR-5/6/7 test relative to the ATR (left) in the northeast flux trap and the individual capsule placement (right).

3. QUALIFICATION TEST DATA

The following data were collected from the AGR 5/6/7 test at Idaho National Laboratory's ATR.

3.1 AGR 5/6/7: Capsule 1 HTIR-TC Data

Capsule 1 in the AGR-5/6/7 fuel test was the bottommost capsule as seen in Figure 1. The placement of the HTIR-TCs can be seen in Figure 2 as a cross-section view of Capsule 1 relative to fuel placement (i.e., large black circles) and other types of TCs (i.e., type N, large orange pentagons, ⬠)—shown here for reference only. Figure 2 also shows a comparison between the temperature measured (in black) by the TCs in Capsule 1 and the theoretically calculated temperature (in red) at the Capsule 1 TC locations. The contour map in Figure 2 is from the calculated expected temperatures of the capsule. This comparison is typical of the Capsule 1 temperature measurements early in the test. The HTIR-TCs are in the hottest region of Capsule 1, with an average measured temperature of about 1300°C.

Due to improper handling, five (5) of the Capsule 1 HTIR-TCs broke during installation. These were classified in the "infant mortality" category and not analyzed further. The other four (4) HTIR-TCs behaved as expected. Their measured temperature data, collected at full reactor power for the entire duration they were operational, are shown in Figure 3.

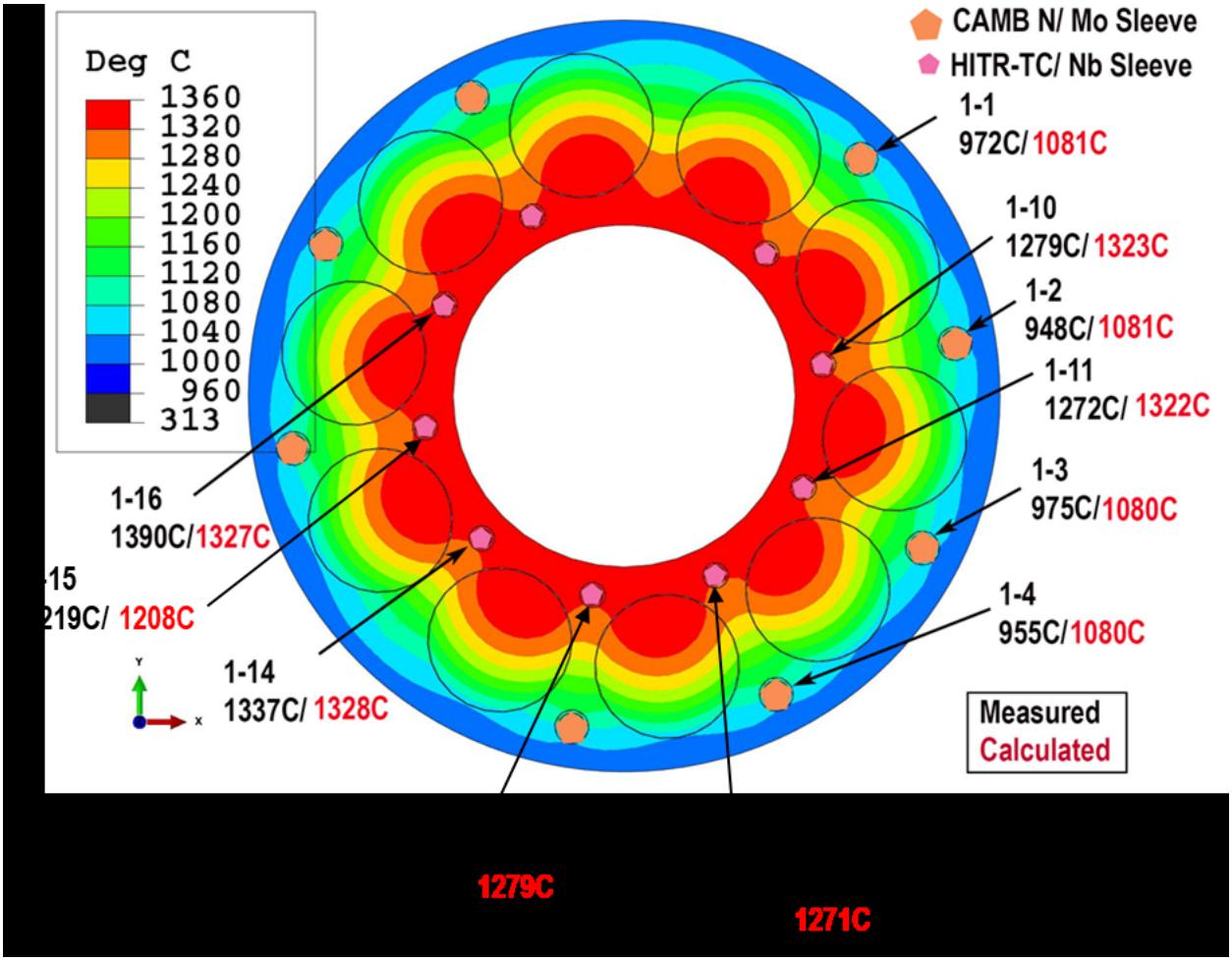

Figure 2. Cross-section view of Capsule 1 with fuel and thermocouple placement. The coloring relates to a snapshot of expected temperatures based on calculations and time.

Figure 3 shows the traces of HTIR-TCs 1-12, 1-13, 1-14, and 1-15 as daily averages. Note that each measured the hottest regions of Capsule 1 by being placed within the inner circle of temperature sensors closer to the fuel. The temperatures measured by these TCs ranged from room temperature to ~1400°C (measured by HTIR-TC 1-14). The data were collected for approximately 425 calendar days, covering the operating life of all the Capsule 1 HTIR-TCs in the AGR-5/6/7 test fixture. The measured operational life in ATR equivalent full-power days (EFPDs) was calculated by noting the duration when the TC was operational, and the ATR reactor was at full power. For HTIR-TCs 1-12, 1-13, 1-14, and 1-15, the operational life was 120, 87, 161, and 120 EFPDs, respectively. The vertical lines found in Figure 3 represent instances in which the ATR was put into shutdown mode and then restarted. However, all the TCs would continue to record temperatures during shutdown mode, regardless.

As shown in Table 1 [8], the theoretically calculated temperatures varied for the different Capsule 1 HTIR-TC locations, but were relatively constant for full-power operation throughout the test.

Table 1. Theoretically calculated temperature at Capsule 1 HTIR-TC locations.

Theoretically Calculated Temperature at Full Power	HTIR-TC 1-12	HTIR-TC 1-13	HTIR-TC 1-14	HTIR-TC 1-15
Temperature [°C]	1271	1279	1328	1208

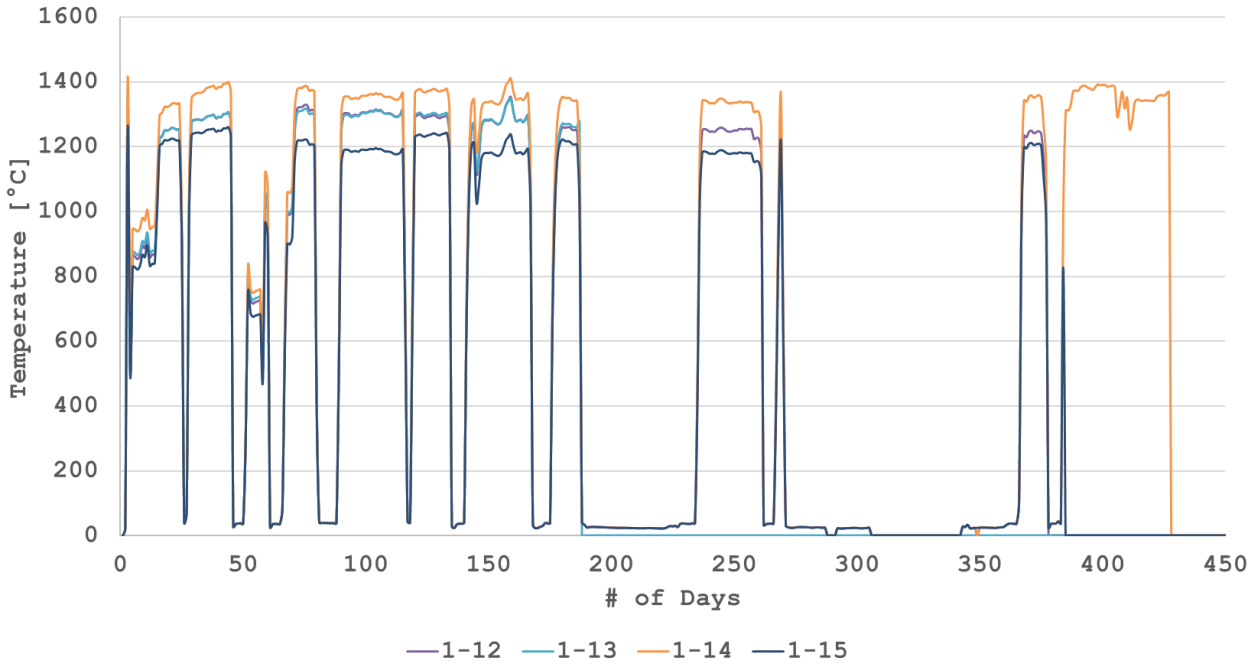

Figure 3. Complete performance of HTIR-TCs 1-12, 1-13, 1-14, and 1-15 in Capsule 1 of the AGR-5/6/7 fuel test.

3.2 AGR 5/6/7: Capsule 3 HTIR-TC Data

Capsule 3 of the AGR-5/6/7 fuel test was centered at the height midplane of the reactor core. The placement of the HTIR-TCs can be seen in Figure 3 as a cross-section view of Capsule 3 relative to fuel placement (i.e., large black circles) and other types of TCs (i.e., type N)—shown here for reference only. Figure 3 also shows a comparison between the temperature measured (in black) by the TCs in Capsule 3 and the theoretically calculated temperature (in red) at the Capsule 3 TC locations. The contour map in Figure 3 reflects the calculated expected temperatures of the capsule. This comparison is typical of the Capsule 3 temperature measurements early in the test. The HTIR-TCs are in the hottest region of the entire test train, and it should be noted that, within this capsule, HTIR-TC 3-5 measured the hottest sustained temperature inside the fuel core test fixture: ~1500°C.

Figure 5 shows the measured temperature data at full reactor power from all three (3) HTIR-TCs in Capsule 3 for the entire duration they were operational. As for Capsule 1, the data were collected for approximately 425 calendar days, covering the operating life of all the HTIR-TCs in Capsule 3 of the AGR 5/6/7 test fixture. The measured operational life in EFPDs was calculated for each HTIR-TC in Capsule 3 by noting the duration when the TC was operational, and the ATR reactor was at full power. For HTIR-TCs 3-5, 3-12, and 3-14, the operational life was 125, 166, and 164 EFPDs, respectively. As in Figure 1, the approximately vertical lines found in Figure 3 reflect the times when the ATR was put into shutdown mode and later restarted. The TCs measured temperature regardless of the reactor state.

As shown in Table 2 [8], the theoretically calculated temperatures varied for the different Capsule 3 HTIR-TC locations but were relatively constant for full-power operation throughout the test.

Table 2. Theoretically calculated temperature at Capsule 3 HTIR-TC locations.

Theoretically Calculated Temperature at Full Power	HTIR-TC 3-5	HTIR-TC 3-12	HTIR-TC 3-14
Temperature [°C]	1436	1327	1185

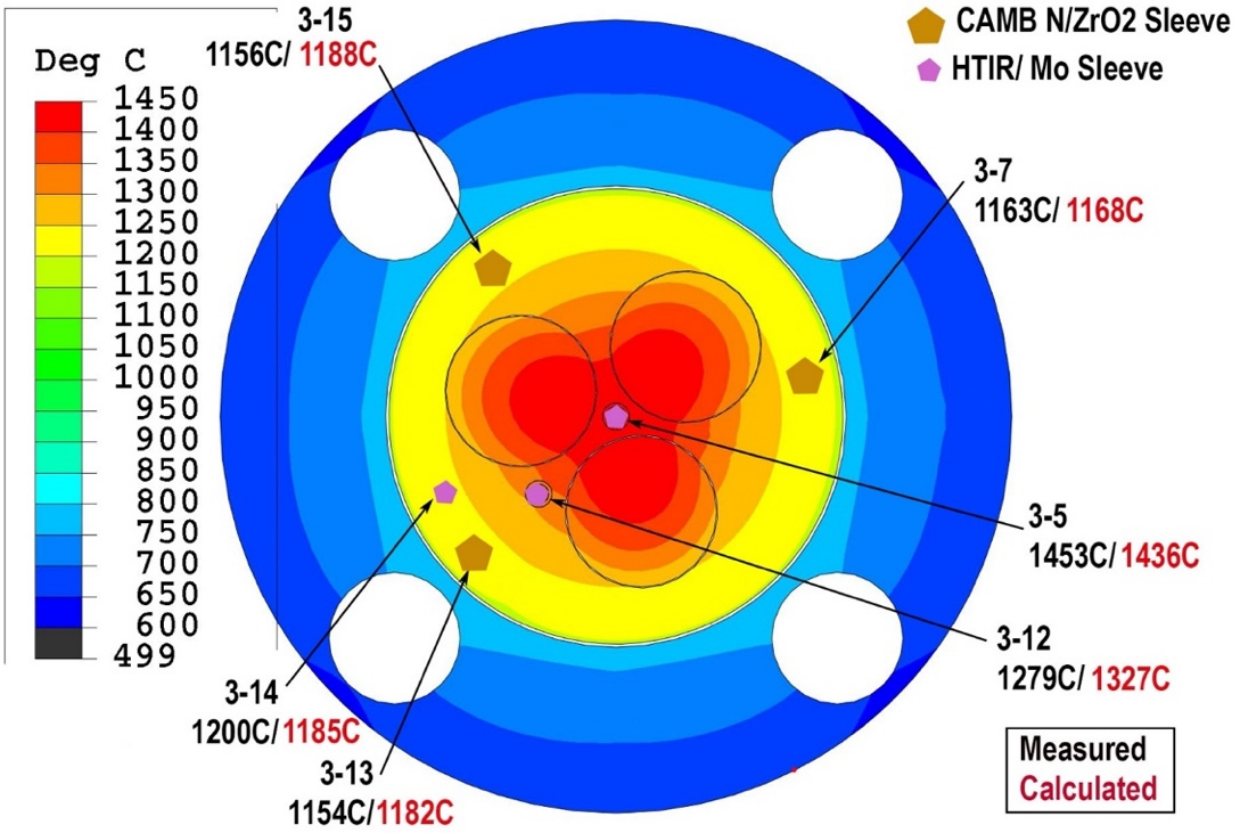

Figure 4. Cross-section view of Capsule 3 with fuel and TC placement. The coloring relates to a snapshot of expected temperatures based on calculations and time.

3.3 AGR 5/6/7: Peak Neutron Flux for Capsules 3 and 1

Table 3 shows the theoretically calculated thermal neutron flux and fast neutron flux (E > 1 MeV) values for full ATR power in the middle of Capsules 3 and 1 (where the HTIR-TC junctions are located) [8]. Note that the neutron flux extends over the whole TC cable and not just the TC junction, and that the radiation effect on the whole cable contributes to the TC reading post-irradiation.

Table 3. Calculated neutron fluxes at the center of Capsules 3 and 1 at full reactor power.

Neutron Flux at Full ATR Power	Capsule 3 (Midplane) [$\times 10^{14}$]	Capsule 1 (Lower Capsule) [$\times 10^{14}$]
Neutron Flux - Thermal (nv)	2.81	1.58
Neutron Flux - Fast (nv)	2.2	1.05

3.4 Effective Power in the ATR Flux Trap Containing the AGR 5/6/7 Test Fixture

Figure 6 shows the effective power of the northeast flux trap during the AGR 5/6/7 test inside the ATR. All power levels are represented, apart from the days in which the reactor was in shutdown mode.

These data show that the power in the flux trap containing the test fixture did not remain constant over the duration of the test, even though the ATR was at full power [9]. The change was ~2 MW, and the average effective power was 16 MW, corresponding to a change of 12.5% (or approximately ±6.3%).

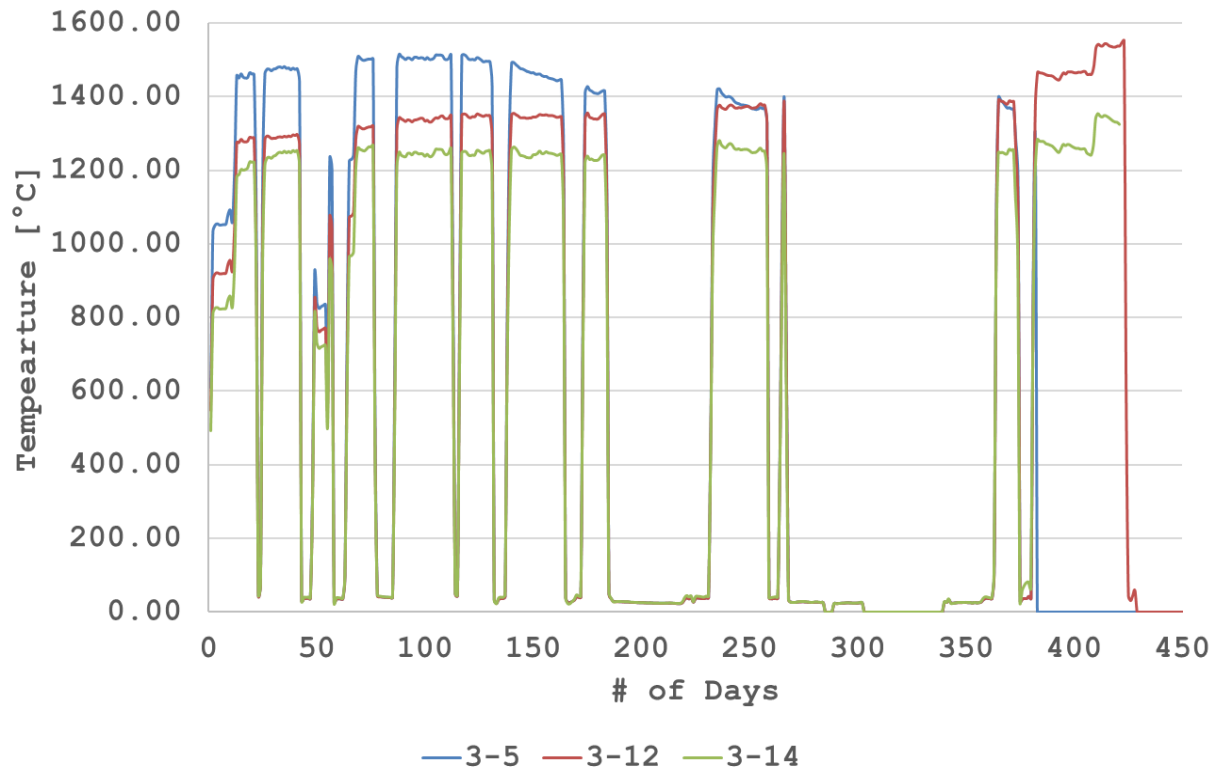

Figure 5. The performance of HTIR-TCs 3-5, 3-12, and 3-14 in Capsule 3 of the AGR-5/6/7 fuel test.

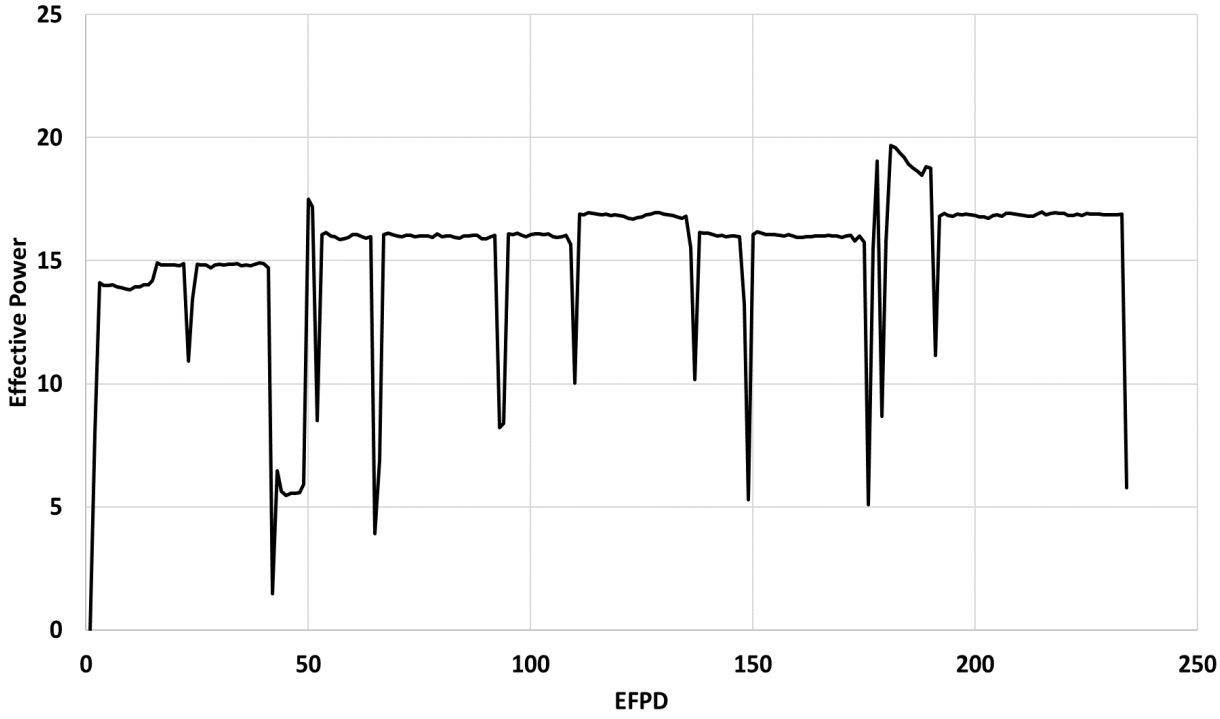

Figure 6. The performance of HTIR-TCs 3-5, 3-12, and 3-14 in Capsule 3 of the AGR-5/6/7 fuel test.

This power change could directly affect the temperature read by the TCs and would cause a synchronous change in all the TC readings. Such a change in the TC readings should not be interpreted as TC drift.

4. QUALIFICATION TEST DATA EVALUATION AND RESULTS

4.1 HTIR-TC Manufacture and Calibration

All HTIR-TCs were manufactured and individually calibrated according to the Qualification Test Requirements [3], as well as according to TEV-2791 [10], issued prior to HTIR-TC installation in the AGR 5/6/7 test.

4.2 HTIR-TC Temperature Measurement Range

The HTIR-TCs accurately measured temperatures ranging from room temperature to the highest temperatures generated in the AGR 5/6/7 experimental test fixture. The highest temperature (both measured and theoretically calculated) was ~1450°C in the center of Capsule 3, as measured by HTIR-TC 3-5. Though the temperature in the experimental test fixture was lower than the HTIR-TC specified maximum temperature of 1600°C, the accuracy of the performance data suggests that the HTIR-TCs could accurately measure temperatures of up to the specified limit of 1600°C in the event the test fixture was designed to produce such a high temperature. However, the drift at that high temperature is uncertain and would have to be measured.

4.3 HTIR-TC Accuracy

The HTIR-TCs used in the AGR-5/6/7 experimental fixture were identically constructed from a consistent batch of individual materials, as per the documented design, manufacture, and processing specifications. A representative sample of ten (10) HTIR-TCs were individually calibrated, and the measured accuracy in the 0–1600°C range was ±1°C or ±0.4% of the temperature reading, whichever was greater, as specified in the Preliminary Calibration Report [4]. This represents the expected, as-manufactured accuracy of the TCs—not to be confused with calibration drift in a neutron flux environment, as discussed in Section 4.5. Note also that the measured accuracy of ±0.4% easily meets the ±1.0% accuracy requirement in the F&OR Report [5].

The AGR-5/6/7 test was not configured to measure the true accuracy of the HTIR-TCs, because it did not contain a calibrated measurement of the temperature. There was a theoretical estimate of the temperature using the ABAQUS finite element model; however, the accuracy of the model is unknown, and the HTIR-TC temperature measurements were used as a validation of the theoretical model. Part of the uncertainty in theoretically calculating the temperature in this experimental fixture is due to the uncertainty in knowing the exact distance of the TC from the core, due to the steepness of the temperature gradient in the fixture. The temperature variance caused by the variance in reactor power in the ATR northeast flux trap containing the test fixture, along with changes in heat-conducting gas composition and flow around the capsules, are other contributing factors. As stated in the Qualification Test Requirements, a ±5% comparison between the temperature predicted by the model and that measured by the HTIR-TC can serve as adequate validation of HTIR-TC accuracy in the AGR 5/6/7 experimental test fixture located in the ATR's neutron flux environment. Noted that this accuracy requirement covers the performance early in the test and does not include the effect of drift due to prolonged residence in a high-temperature, high-neutron-flux environment, as is covered in Section 4.5.

4.3.1 HTIR-TC Accuracy in Capsule 3

Placed in the center of Capsule 3's hot zone, HTIR-TC 3-5 measured around 1453°C for the first few weeks of operation at full reactor power. The theoretically calculated temperature at that location, based on thermal models, was 1436°C. The difference is 17°C or ~1.2% higher than the modeled temperature. This is in good agreement with the 1% HTIR-TC accuracy requirement, since the accuracy of the temperature calculated by the thermal model is believed to be ~5%. Table 4 shows a comparison between all the Capsule 3 HTIR-TC temperature readings and the temperatures predicted by the thermal model.

Capsule 3 contained three (3) type N TCs in the same lower temperature zone as HTIR-TC 3-14, and all three gave similar temperature measurements—further evidence of HTIR-TC accuracy at this lower temperature. The type N TCs are shown for comparison but can physically only measure up to 1260°C (or 1280°C for a very short period), since that approaches the type N melting point restrictions. On the other hand, the HTIR-TCs can measure accurately at up to 1600°C.

Table 4. Capsule 3 measured vs. calculated temperature results.

Capsule	HTIR-TC #	Measured Temperature [°C]	Calculated Temperature [°C]	Difference [°C]	Difference [%]
3	3-5	1453	1436	17	1.2
3	3-12	1278	1327	-49	-3.6
3	3-14	1200	1185	15	1.3

Table 5 shows comparisons between measurements made by HTIR-TC 3-14 and the type N TCs placed in a similar location.

Table 5. Capsule 3 comparison of type N vs. HTIR-TC.

Capsule	HTIR-TC #	Measured Temperature [°C]	Calculated Temperature [°C]	Difference [°C]	Difference [%]
3	3-14	1200	1185	15	1.3
–	Type N #	–	–	–	–
3	3-7	1163	1168	-5	-0.4
3	3-13	1154	1182	-28	-2.4
3	3-15	1156	1188	-32	-2.7

4.3.2 HTIR-TC Accuracy in Capsule 1

Capsule 1 contained four (4) operating HTIR-TCs around the perimeter of the test fuel. These measured slightly lower temperatures than those in Capsule 3. A comparison between these HTIR-TC temperature readings and the temperatures predicted by the thermal model is shown in Table 6.

Table 6. Capsule 1 measured vs. calculated temperature results.

Capsule	HTIR-TC #	Measured Temperature [°C]	Calculated Temperature [°C]	Difference [°C]	Difference [%]
1	1-12	1250	1271	-21	-1.7
1	1-13	1250	1279	-29	-2.3
1	1-14	1323	1328	-5	-0.4
1	1-15	1219	1208	11	0.9

These results also show the difference to be within the 5% expected error band of the theoretical model calculations.

The constancy of the measured temperatures for the HTIR-TCs in Capsules 3 and 1 early in life (prior to any appreciable TC drift) indicates that, although the agreement between the measured and calculated temperatures was only 5%, this error band is indicative of the error in the theoretical temperature estimate

and variation in reactor power, and the HTIR-TCs were reading the actual temperature at their locations within the specified accuracy of 1%.

4.4 HTIR-TC Repeatability

During the ATR AGR-5/6/7 test, HTIR-TC test data were collected and analyzed over a period of several calendar months. During this time, the reactor operated at 100% power for certain periods but was also shut down from 100% power and then brought back up to 100% power several times, with these shutdown periods lasting anywhere from a few days to approximately 25 days. This provided good data for checking the HTIR-TCs' repeatability by verifying whether they returned to the same temperature after reactor shutdown and restart. An examination of Capsule 1's HTIR-TC-measured temperature data (see Figure 3) and Capsule 3's HTIR-TC-measured temperature data (see Figure 5) reveals that all HTIR-TCs, operating in different temperature zones at 100% power, recover to their pre-shutdown value once the reactor starts back up and returns to 100% power. For each TC, there is a slight variation in the measured temperature at 100% power, but this is likely due to a change in reactor power, since the variations in the TC measurements are synchronized and simultaneously appear for all the TCs.

4.5 HTIR-TC Drift Data

Figure 7 and Figure 8 show a plot of the HTIR-TC temperature measurements for Capsules 1 and 3, respectively. These figures were derived from the data in Figure 3 and Figure 5 by discarding the reactor down time. The data, however, have not been corrected for any apparent drift by discounting significant synchronized changes due to power or ambient temperature changes.

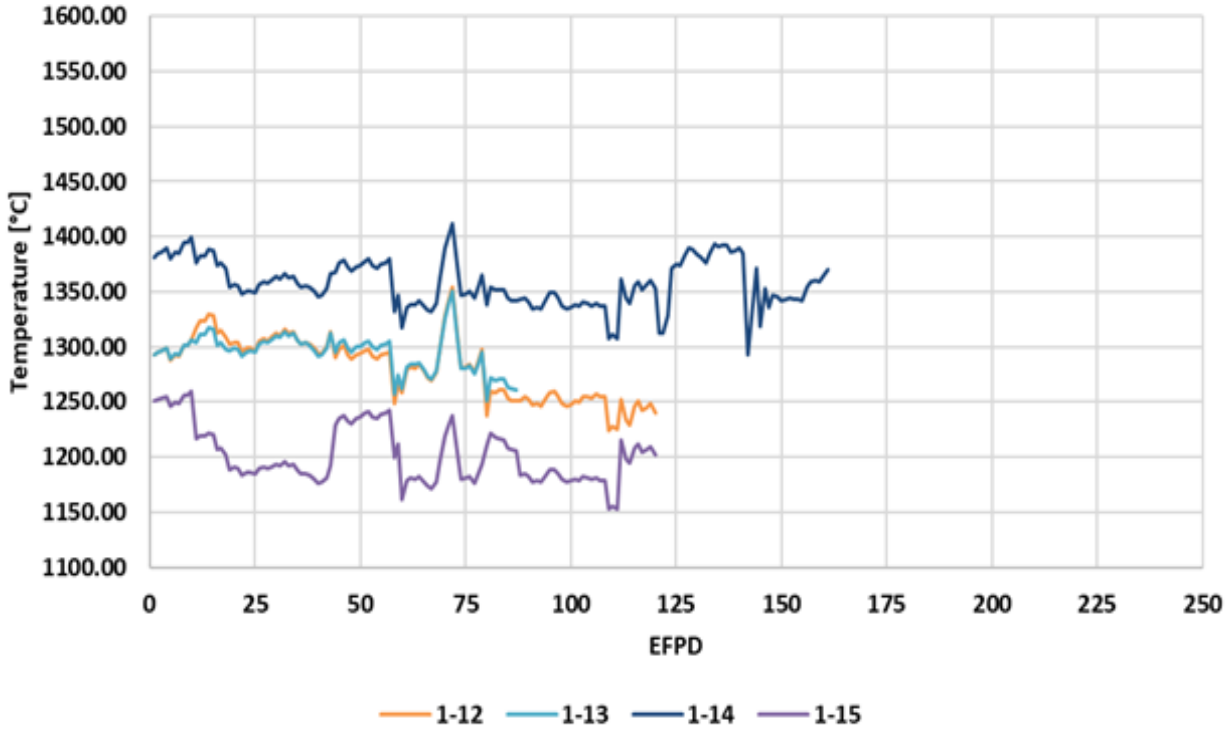

Figure 7. HTIR-TC temperature measurements for Capsule 1.

4.5.1 Capsule 1 HTIR-TC Trends

The data in Figure 8 show that the four HITR-TCs in Capsule 1 appeared to experience a small downward drift of 3–4% for an ATR residence time of 150 EFPDs, but this could not be well quantified over the noise in the data, due to experimental error. The noise in the data was approximately ±2% and appeared to be synchronized, implying it was caused by changes in the ambient temperature and not

changes in the TC response. This trend as a function of time is shown more clearly in Figure 9, where the TC measurements are normalized to their initial value. A type N TC is also shown for comparison. Only one type N TC is shown in Figure 10, since the other type N TC in Capsule 1 demonstrated abnormally noisy performance that would distract from the current discussion.

These data show that the HTIR-TCs in Capsule 1 performed as expected, and that the downward drift over the thermal and fast neutron fluence level corresponded to 125 EFPDs. Operation for that length of time at a high temperature of 1280°C was generally within the specified value of 3.5%. These HTIR-TCs met the specified requirement for drift caused by thermal and fast neutron irradiation in the ATR.

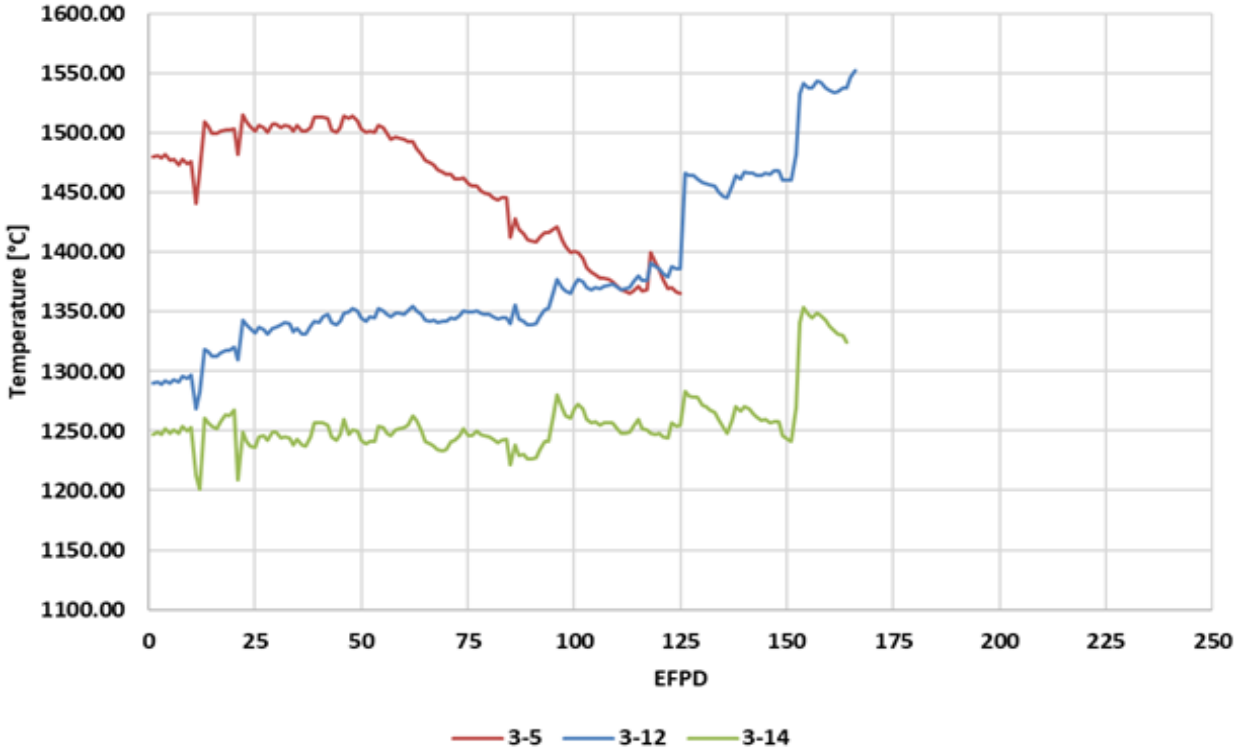

Figure 8. HTIR-TC temperature measurements for Capsule 3.

4.5.2 Capsule 3 HTIR-TC Trends

The data in Figure 9 show different temperature measurement trends for the three (3) HTIR-TCs in Capsule 3—3-14, 3-12, and 3-5. HTIR-TC 3-14 showed no change in trend, either up or down, while 3-12 showed an upward trend. An examination of other type N TCs in a Capsule 3 temperature location similar to that of 3-12 also revealed the same upward trend. HTIR-TC 3-5, on the other hand, showed a significant downward trend. These trends as a function of time are shown more clearly in Figure 10, with the TC measurements normalized to their initial value.

These data indicate that the noise in the measured temperatures for all TCs is synchronized, meaning that these changes do not reflect a true drift of the TCs but rather a trend indicative of the changes in the temperature environment.

Figure 9. Temperature measurements taken by HTIR and type N TCs in Capsule 1 of AGR 5/6/7. Normalized by the initial temperature measurement in-situ, T_{INT}. The HTIR-TCs are in color, the type N TC (1-4) in black.

Figure 10 reveals the three types of measured temperature trends exhibited by TCs in Capsule 3:

1. The first trend is the relatively constant temperatures exhibited by HTIR-TC 3-14 and type N TCs 3-2, 3-13, and 3-15 for up to 150 EFPDs. Note in particular that type N TC 3-13 was the "control" TC for the entirety of the experiment, meaning that the reactor power and gas flow mixture was adjusted based on the temperature readings of TC-3-13. After 150 EFPDs, a synchronized increase in temperature was noted by all the TCs, indicating a sudden increase in ambient temperature.
2. The second trend is that a cluster of TCs (specifically HTIR-TC 3-12 and type N TCs 3-1, 3-3, and 3-4) all showed a gradual increase in measurement readings with time, beyond the TCs specified life and up to 175 EFPDs. There is no physical reason for the TC sensitivity to increase synchronously for this entire group of HTIR-TCs and type N TCs. This increase is not due to TC sensitivity change (i.e., drift), but rather that the ambient temperature in this region of Capsule 3 was gradually heating up. It is also likely that this increase in ambient temperature more than cancelled the expected downward drift due to transmutations. The reason for this increase is not well understood, but likely relates to the difficulty of maintaining a constant temperature for the Capsule 3 design. One reason TCs 3-1, 3-3, and 3-4 are trending up is because this capsule has two graphite layers and these three TCs are in the outer layer. As the fuel powers down, there is less heat flux moving from the fuel to the capsule wall—which is cooled by water. To maintain a constant temperature in the fuel, a larger temperature increase begins to manifest between the wall and the first layer of graphite. So these three TCs should climb in temperature as the fuel continues to power down. A second source of the temperature rise comes from a change in the concentration of He and Ne gases flowing through the capsule to maintain a constant temperature and could affect an increase in the ambient temperature read by the TCs. Thirdly, examination of the experimental test data showed that the TC used to control the ambient temperature (i.e., TC-3-13) was losing sensitivity, which would cause an increase in Capsule

3's ambient temperature.

3. The third trend pertains to the measurements from HTIR-TC 3-5. As the only TC located in the center of Capsule 3, HTIR-TC 3-5 had no other similarly located TCs to compare against. HTIR-TC 3-5 showed a relatively constant reading up to approximately 75 EFPDs, at which point the reading started to decrease, leading to a 125°C change (-8.7%) at 125 EFPDs. If, as suggested by the data for HTIR-TC 3-12 and the other type N TCs, the capsule was heating up, then the downward drift could

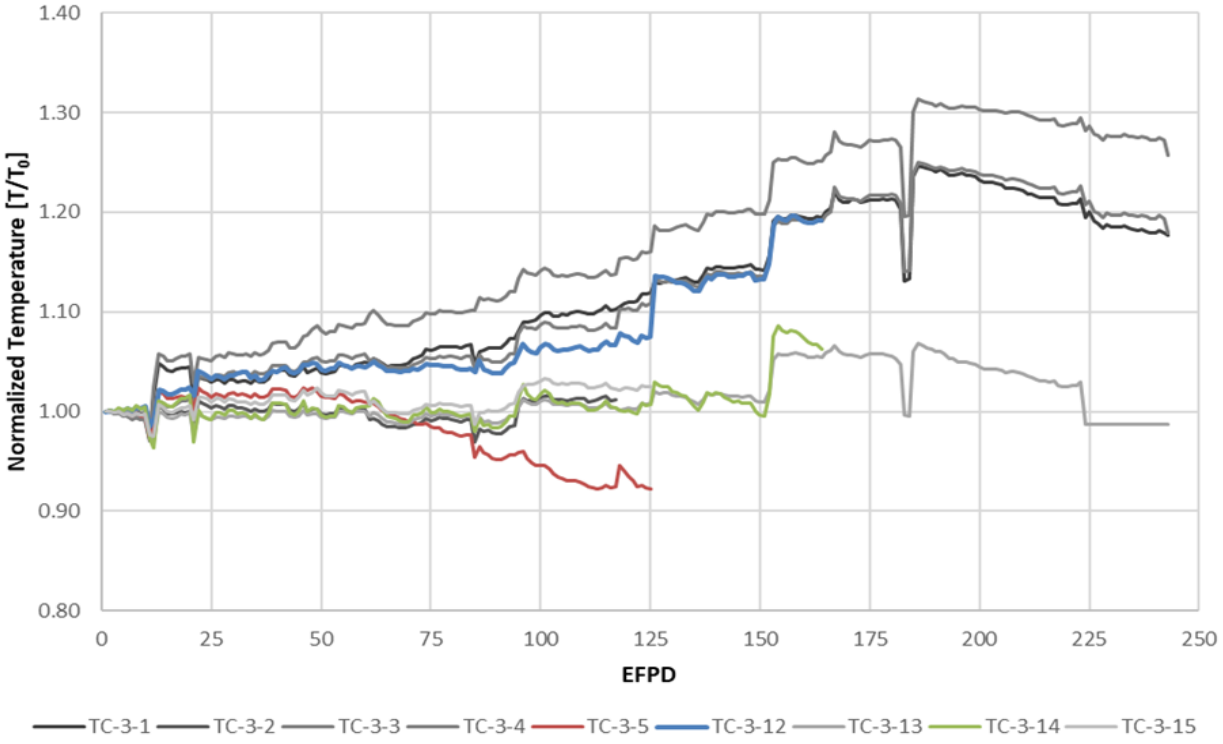

Figure 10. Measurements taken by HTIR and type N TCs in Capsule 3 of AGR 5/6/7. Normalized by initial the temperature measurement in-situ, T_{INT}. The HTIR-TCs are in color, the type N TCs in grayscale.

actually be larger than 10%. It is unlikely that this large downward drift was due to a large temperature decrease at this location. It is also unlikely that fast neutron damage or thermal neutron transmutations could have caused this effect, since the cables of all Capsule 1 and 3 HTIR-TCs saw similar thermal and fast neutron fluxes and did not register this large downward drift. It is more likely that the drift is due to a real decrease in the TC sensitivity. The reason for this large downward drift is believed to be caused by prolonged residence time at high temperature (~1500°C). Several possible effects can arise from operating at this high temperature:

a. It is possible that, although this TC was heat treated to 1450°C for several hours during manufacture, it needed to be heat treated at a higher temperature for a longer time in order to stabilize the grain structure for long-term operation at higher temperatures (1500°C). The experience related in the literature shows that TC sensitivity can decrease if the grain structure is not stabilized prior to operating above processing temperature for long periods of time.

b. It is possible that impurities diffused into the thermoelements at this high temperature. For example, Figure 8 shows that HTIR-TC 3-5 initially operated, on average, at 200–300°C hotter than the other HTIR-TCs in Capsule 3. Although this TC, like all the others, was heat treated at 1450°C in the calibration environment, it is possible that,

within the test fixture and nuclear environment, additional impurities permeated into the thermoelements over time via solid-state diffusion at this higher operating temperature.

These data reveal the difficulty of determining TC drift in this ATR test fixture and comparing it with drift specifications, due to the potential change of ambient temperature in Capsule 3. With the exception of HTIR-TC 3-5, it is likely that, if the temperature did not change, the other Capsule 3 HTIR-TCs—operating at lower temperatures than HTIR-TC 3-5—would meet the specification of <3% downward drift at 125 EFPDs in the ATR test fixture. HTIR-TC 3-5, which was located in the hottest region, had an anomalously high downward drift caused by operating at a temperature higher than its heat treatment temperature. This caused insufficient metallurgical grain structure stabilization, or significantly higher diffusion of impurities into the TC junction.

4.6 HTIR-TC Drift Analysis

In general, calibration drift of an in-pile reactor TC arises from the temperature and radiation effects of the thermoelement materials, as well as from the potential introduction of impurities and changes in metallurgical grain structure by prolonged operation at high temperature. For HTIR-TCs, their entire lengths—as well as that of the cables—in the hot reactor are heat treated at high temperature prior to use, thus minimizing any HTIR-TC calibration changes due to potential changes in the thermoelement Seebeck coefficients, as a result of long-term exposure at high temperature. However, based on previous experiments with Mo/Nb TCs, drift occurs even when the heat treatment temperature is higher than the operating temperature [11]. However, this temperature-dependent drift becomes negligible if the heat treatment temperature is more than 400°C higher than the operating temperature.

The capsules are designed so that the TC cables are routed through the cooler regions of the capsules, where the temperature is at least 300°C lower than the heat treatment temperature. However, the TC cables see the full neutron flux at their axial locations independent of the temperature. The drift due to neutron flux is generated through this length of the TC cable, while the drift due to prolonged high-temperature operation is due mainly to a relatively short section of the TCs in the capsule being exposed to high temperatures.

Basically, three effects can alter the TC Seebeck coefficient and cause drift:

1. Transmutation of the thermoelements by neutron absorption primarily through thermal neutrons, since they have a significantly higher cross section than fast neutrons. TCs with transmuted elements have a different Seebeck coefficient than the original, and this causes TC drift, which increases with thermal neutron exposure ($nvt_{thermal}$).
2. Change in the lattice structure of the thermoelements, due to bombardment (primarily by fast neutrons). The changed lattice structure also alters the Seebeck coefficients and results in TC drift, which increases with fast neutron exposure (nvt_{fast}).
3. Prolonged operation at high temperature, which can change the metallurgical grain structure of the material and introduce impurities into the TC.

For the HTIR-TCs in the ATR test fixture, the drift due to neutron fluence is mainly caused by exposure of the TC wiring in the neutron flux field, and not the actual junction where the measurement is taking place, since the TC electromotive force (EMF) is being generated along the length of the wires (where there are thermal gradients). Note that changes in temperature along the cables generate EMF but do not affect TC calibration or drift as long as the Seebeck coefficient of the thermoelements does not change. However, transmutations and changes in the lattice structure due to neutron bombardment can alter the Seebeck coefficients and thus change the HTIR-TC calibration [12].

The drift due to prolonged operation at high temperature is dependent on what the operating temperature is compared to the temperature at which the TC was heat treated during the manufacturing process. The more the heat treatment temperature exceeds the operating temperature, the smaller the change in material structures and Seebeck coefficients as a result of this cause.

Changes to the Seebeck coefficient as a result of these three causes changes the TC response and the response recorded during the calibration test prior to sensor installation [5]. The changes are gradual with respect to neutron exposure and time at high temperature and appear as drift in the TC reading.

Though these Seebeck coefficient changes due to irradiation are small, they are too complex to calculate theoretically, and so must be calculated based on the experimentally observed drift data. The best experimental drift data come from the HTIR-TCs in Capsule 1, since no significant changes in temperature occurred in Capsule 1. The drift data from the HTIR-TCs in Capsule 3 are not as reliable, since significant changes in temperature occurred in Capsule 3. Experimental data showed that the HTIR-TCs in Capsule 1 drifted down by approximately 3.5% after 125 EFPDs in the ATR test fixture. Therefore, the HTIR-TC Drift Model's Seebeck coefficient degradation constants for thermal and fast neutron fluence, and for prolonged operation at high temperature, need to be adjusted to match the observed downward drift of ~3.5% at 125 EFPDs for the Capsule 1 HTIR-TC (1-14) operating at ~1280°C, as well as the downward drift of ~8.7% at 125 EFPDs for the Capsule 3 HTIR-TC (3-5) operating at ~1500°C. Also, the thermal flux degradation constant should be such that it produces an acceptably low downward drift of <1% in a commercial power reactor, for a thermal neutron exposure of 3.8×10^{21} nvt, which corresponds to a typical 18-month refueling cycle outage.

The following general factors apply to our understanding of the drift that results when HTIR-TCs in the ATR test fixture are exposed to neutron fluxes and high temperatures:

1. Neutron-fluence-induced TC drift is due primarily to neutron-fluence-induced transmutations and neutron bombardment effects in the thermoelement cables. These effects cause the Seebeck coefficient to change as a function of residence time in the reactor and occur in the region which the temperature changes. Thus, for constant temperature profiles, the drift in Capsule 1 TCs is mainly caused by the neutron fluence effects in Capsule 1 cables as they pass through the large temperature change region of Capsule 1; the smaller temperature changes in the cable transport regions of Capsules 2–5; and the cooler regions between Capsules 1-2, 2-3, 3-4, and 4-5. Similarly, the drift in the Capsule 3 TCs is caused by neutron fluence effects in Capsule 3 cables as they pass through the high-temperature change region of Capsule 3, the smaller temperature change in the cable transport regions of Capsules 4 and 5, and the cooler regions between Capsules 3-4 and 4-5. Note that since the temperature fluctuations in these in-between capsule regions are approximately equal, the EMF generated in the TC cables in these regions tend to cancel each other out and do not significantly affect the measured TC EMF prior to irradiation. However, after irradiation, the Seebeck coefficient in various parts of the cables is affected differently, since the neutron fluxes are different in different cable regions and the EMFs due to temperature fluctuations do not cancel each other out and must be computed for accurate drift data analysis. The Seebeck coefficient change due to neutron fluence can be estimated from theoretical considerations backed by experimental, data as described in the HTIR-TC Drift Model (Section 4.6.1).
2. Drift due to prolonged operation at high temperature is caused by a change in the Seebeck coefficient of the HTIR-TC in the capsule's high-temperature region, in which the difference between the operating temperature (T) and the heat treatment temperature (T_0) is greater than the given value determined by the TC design ($T - T_0 < \sim 400$°C for HTIR-TC). When $T-T_0 > -400$°C and $T<T_0$, the drift increases as T approaches T_0 and increases dramatically when $T>T_0$. The change in the Seebeck coefficient due to this effect can be estimated from the experimental data on drift as a function of time of operation at high temperature, as described in the HTIR-TC Drift Model (Section 4.6.1). There is negligeable change in the Seebeck coefficient in the rest of the TC cable outside the capsule because the temperature in these regions is well below the heat treatment temperature.

According to the requirement in the F&OR report [1], neutron-fluence-induced drift for a standalone HTIR-TC application in a commercial power reactor must be less than approximately -1% of the measured temperature for 18 months and a conservatively estimated thermal neutron exposure of 3.8×10^{21} nvt, corresponding to an average thermal neutron flux of approximately 8×10^{13} nv. Similarly, the drift requirement for a 24 months cycle with the same neutron flux would be -1.5%. A drift of < -1%

for 18 months (or -1.5% for 24 months) of reactor operation is considered acceptable for installing the HTIR-TC as a standalone TC in a light-water power reactor (e.g., boiling-water reactor [BWR] or pressurized-water reactor [PWR]) where the thermocouple would be used primarily for high temperature measurements in case of an accident. The drift of the HTIR-TC in the ATR AGR-5/6/7 test fixture was specified at a higher value (3.5%) for 125 EFPDs because, in addition to drift due to neutron fluence, there is also drift due to prolonged operation at high temperature. A HTIR-TC Drift Model was developed that uses calculated temperature and neutron flux profiles to calculate drift due to neutron fluence, and it uses experimentally measured drift at high temperature (no radiation) to estimate the expected high-temperature drift in the ATR test fixture. The Drift Model produces results that approximately match the observed drift data in the ATR qualification test, and also extrapolates to approximately match the drift data available in the literature.

4.6.1 HTIR-TC Drift Model

A model and general procedure for calculating HTIR-TC drift in the ATR AGR-5/6/7 test fixture were developed. These are described briefly in the steps below (for drift due to neutron fluence and drift due to prolonged operation at high temperature):

4.6.1.1 *Model for Drift Due to Neutron Fluence*

Using the following theoretical temperature calculations, determine the temperature profiles in all sections of the HTIR-TC thermoelement cables in the reactor where they are subject to drift due to neutron bombardment:

1. Estimate the high temperatures read by the TC tips in the approximate mid-region of Capsules 1 and 3 where the HTIR-TCs are located.
2. Estimate the slight reduction in temperature as the cables reach the exit of the capsule.
3. Estimate the sharp decrease in temperature as the cables enter the gap between the capsule and the neighboring capsule, where they are cooled by the He-Ne gas mixture flowing near the edges of the capsules.
4. Estimate the increase in temperature as the cables enter and travel through the cable bypass region of the upper neighboring capsule, where they are heated by the capsule's high temperature while also being cooled by the flowing, He-Ne gas mixture.
5. Estimate the decrease in temperature as the cables leave the cable bypass region of the neighboring capsule and enter the gap region between the upper neighboring capsules.
6. Repeat Steps 4 and 5 and estimate the cable temperatures as the cables pass through all the in-between capsule regions and finally reach the top-most capsule (i.e., Capsule 5).
7. The temperature then decreases to the reference ice temperature (0°C).
8. The results of this temperature profile calculation are shown in Section 4.6.2.

For the drift calculation, it is assumed that the temperature profiles for the HTIR-TCs in Capsules 1 and 3 are constant for all EFPD and do not change with time/residence in the reactor.

After the temperature profile of the entire length of TC cable is determined the local Seebeck coefficient needs to be estimated. The following show the steps for estimating the local Seebeck coefficient prior to irradiation:

9. The HTIR-TC Drift Model determines the TC's EMF by integrating the Seebeck coefficient multiplied by the change in temperature with respect to distance over the length of the cable, as per the following equation:

1

where:

x = Distance along the TC cable [ft], measured from the top of the reactor.

$S_{eff}(T,x)$ = Effective Seebeck coefficient of the Mo/Nb TC [mV/°C], which is a function of the temperature. And since the temperature varies along the TC wires, it is also a function of distance along the TC wires.

dT/dx = Rate of temperature change with distance [°C/ft].

L = Full length of TC cable [ft].

Note that, since each thermoelement generally has its own Seebeck coefficient, S(T), in this equation is the combined or effective Seebeck coefficient, $S_{eff}(T,x)$, of the Mo and Nb thermoelement wires, and is equal to the difference between the Seebeck coefficients for Mo and Nb. The Seebeck coefficient for Mo, $S_{Mo}(T,x)$, is positive for all temperatures, and its magnitude is much larger than the Seebeck for Nb, $S_{Nb}(T,x)$. On the other hand, $S_{Nb}(T,x)$ is negative at low temperatures and positive at high temperatures, and its magnitude is significantly less than $S_{Mo}(T,x)$ at all temperatures. The value of $S_{eff}(T,x)$ varies with temperature and is positive for all temperatures in the measurement range. The magnitude of $S_{eff}(T,x)$ slightly varies for each HTIR-TC and depends on the heat treatment of the TC as well as on the thermal and fast neutron fluence it eventually undergoes in the reactor. The $S_{eff}(T,x)$ value can be estimated from the literature but is more accurately estimated from the test data using the HTIR-TC Drift Model.

10. Determine the unirradiated effective Seebeck coefficient as a function of temperature. Note that, since the HTIR-TCs were individually calibrated after heat treatment, the unirradiated effective Seebeck coefficient, $S_{eff}(T,x)$, as a function of temperature and distance can be determined from the HTIR-TC calibration data. Numerically, this is the slope (or tangent) of the measured voltage [mV] vs. temperature [°C] polynomial curve at various temperatures. A polynomial can be fit to this data so that the unirradiated effective Seebeck coefficient can be determined for all temperatures in the measurement range. That is, $S_{eff}(T,x)$ equals a polynomial fit of dV/dT as function of temperature, based on the HTIR-TC calibration data. Results of this unirradiated effective Seebeck coefficient calculation are shown in Section 4.6.2. The Seebeck coefficient is then used as follows to calculate the total EMF generated in the thermoelements:

2

11. By integrating Equation 1, determine the unirradiated EMF of the HTIR-TCs found in Capsules 1 and 3 of the test fixture. This integration is done numerically by dividing the TC length into small-distance increments, determining the temperature change by referring to the temperature profile obtained in Step 1, then multiplying by the average unirradiated effective Seebeck coefficient for that temperature and spatial increment from Step 3 in Section 4.6.1 to give the incremental EMF generated by that small incremental distance. Next, add up the incremental EMFs for the whole TC length. This value should approximately equal the measured EMF value for that temperature in the calibration test.

Now the effect of irradiation on the TC thermoelements of Mo and Nb—and in turn the Seebeck coefficient—must be estimated by a reduction factor considering the thermal and fast neutron profiles:

12. Determine the thermal neutron and fast neutron flux profile across all capsules, based on ATR documentation and modified by experimentally determined factors for the test fixture.

13. Estimate the effective Seebeck coefficient reduction due to thermal and fast neutron irradiation. The HTIR-TC Drift Model assumes that the Seebeck coefficient reduction due to neutron fluence has the following form:

, 3

where $C_{1\&2}$ are the correction factor coefficients for both thermal and fast neutrons, respectively; φ is the neutron flux for thermal and fast neutrons (as shown); and t is the total irradiation time. This

brings the Seebeck coefficient, reduced by nuclear irradiation, to a new irradiated Seebeck coefficient, $S^*(T,x)$, where the * represents the reduced, irradiated version:

4

A conservatively high estimate of the neutron flux reduction factor constant, C_1, for thermal flux is obtained by first adding the 2200 m/sec thermal neutron absorption cross section of the Mo and Nb, where the Mo absorption coefficient is the sum of the absorption coefficients of the Mo isotopes weighted by their fractional abundance (2.48 barns), and the Nb cross section is 1.48 barns (see the F&OR report). Thus, the conservatively high thermal neutron 2200 m/sec cross section of the Mo/Nb TC is 3.63 barns. The reason for choosing a conservatively high value for the 2200 m/sec thermal neutron absorption cross section is to provide a conservatively high drift estimate for HTIR-TC application in a commercial BWR or PWR, where the neutron flux is primarily thermal. The constant C_1 is then obtained by converting this 2200 m/sec cross section (corresponding to an average thermal neutron temperature of ~ 20°C) into the cross section at the average ATR thermal neutron temperature of 60°C. The constant C_2 for fast flux is generally much smaller than C_1 for thermal flux, and for the Drift Model is assumed to be 0.5 barns.

Using $S^*_{eff}(T,x)$, the effective EMF from irradiated TCs is then calculated using the method similar to Step 11 as follows:

14. Determine the irradiated EMF of the Capsule 1 and Capsule 3 HTIR-TCs in the test fixture by numerically integrating the incremental EMF values for the irradiated TC. Note that this irradiated EMF is due only to the reduction in Seebeck coefficient due to the thermal and fast neutron fluence and does not include the change in Seebeck coefficient due to prolonged operation at high temperature. The incremental EMFs for the irradiated TCs are calculated by multiplying the incremental temperature change for each incremental distance along the TC by the reduced effective Seebeck coefficient at that location and temperature. The incremental EMFs are added together to give the total irradiated EMF:

. 5

15. The HTIR-TC drift due to neutron fluence calculated by the Drift Model is then calculated using the EMF generated from unirradiated and irradiated thermoelements as follows:

. 6

4.6.1.2 *Model for Drift Due to High Temperature Operation*

In the past, experiments were conducted in test ovens to determine the HTIR-TC drift caused by operation at high temperature, leaving out drift due to reactor neutrons. These experiments proved that drift occurred, and that it was due to changes in the TC's metallurgical structure as well as the potential introduction of impurities into the TC. The data and cause of this drift suggest that the drift depends on the difference in between the TC heat treatment temperature (T_0) and operating temperature (T), and drift can occur whenever T is less than T_0. The greater the temperature difference (T_0 - T), the less the drift; and the less the temperature difference, the greater the drift.

Determine High-Temperature Drift Data

Figure 11 shows typical raw data for the measured temperatures of the HTIR-TC and type K and N TCs as a function of time and at a constant oven temperature [11].

The data show that every TCs measuring a high temperature of ~1200°C showed drift. The drift was more severe for the type K and type N TCs than for the HTIR-TCs; however, for HTIR-TCs heat treated at 1500°C, the drift at 1200°C for 4000 hours was still significant: ~1.6%. The data also show that, after a

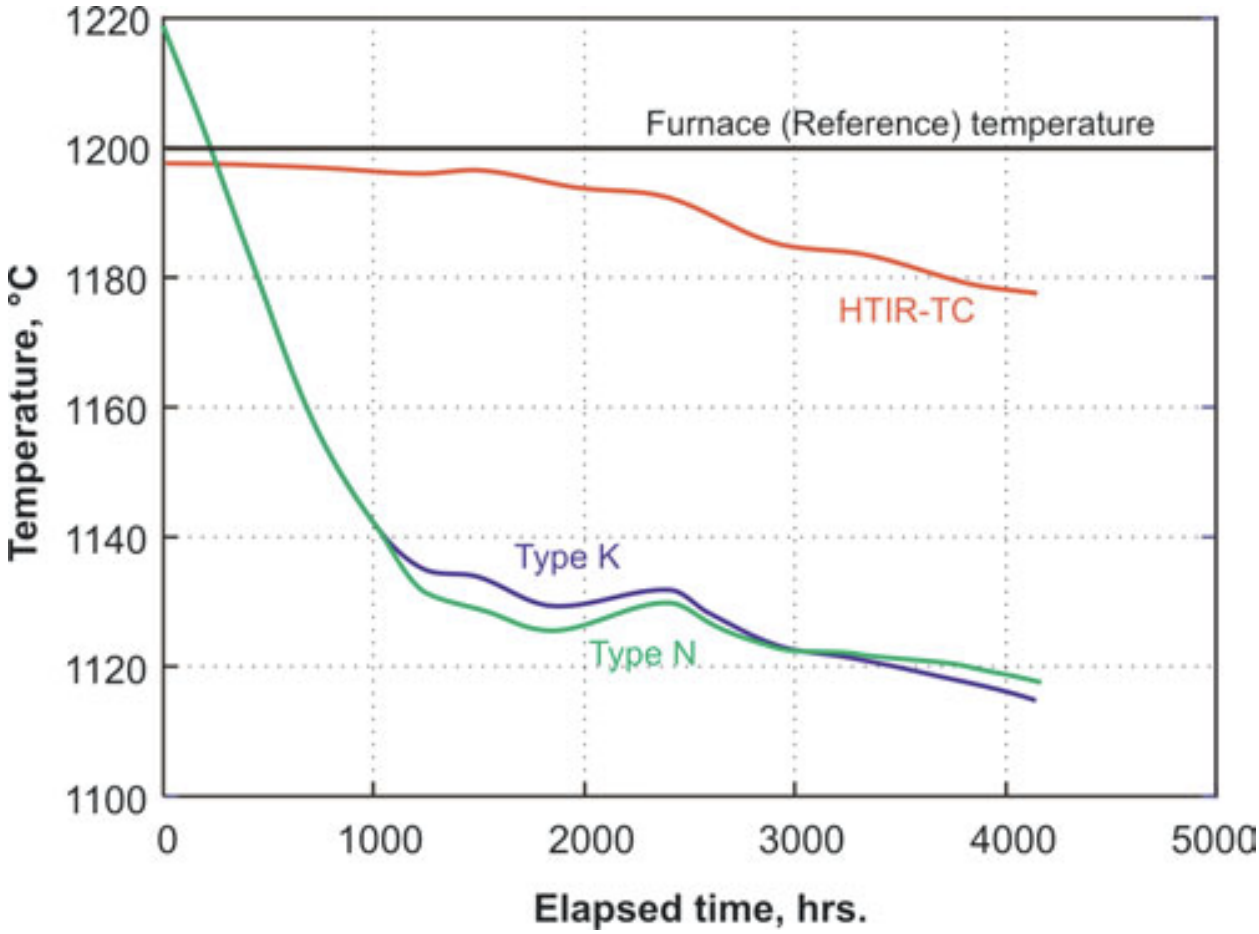

Figure 11. Experimental data for drift due to high-temperature operation [11].

severe drop, the drift levels off at some maximum value. This is technically understandable, since the TC is not expected to continue to drift after the metallurgical structure has stabilized at the operating temperature.

Determine High-Temperature Drift for HTIR-TC ATR Test

Convert the temperature drift data in Figure 11 to relative drift as a function of time, then draw an approximate smooth curve to adequately cover the data obtained through 3000 hours, which is equivalent to the 125 days for which the drift in ATR is to be determined. Note that these drift data were based on a heat-treatment/operating temperature difference of 1500 - 1200 = 300°C. The drift data are then extrapolated to a temperature difference of 1450 - 1293 = 157°C to match the temperature difference between HTIR-TC 1-12 and 1-13, then extrapolated to a temperature difference of 1450 - 1381 = 169°C for HTIR-TC 1-14, and to a temperature difference of 1450 - 1500 = -50°C to match the temperature difference for HTIR-TC 3-5. For these extrapolations, it is necessary to ensure that, when adding the extrapolated high-temperature drift at 3000 hours to the neutron fluence drift for 3000 hours, the result approximately matches the observed 3000-hour (125 EFPDs) ATR test drift of -3.3% for HTIR-TC 1-12 and 1-13, -3.7% for HTIR-TC 1-14, and -8.7% for HTIR-TC 3-5. The Drift Model also assumes that, when the operating temperature is more than 400°C below the heat treatment temperature, the drift due to high-temperature operation becomes negligeable.

4.6.1.3 *Model to Calculate Total Drift for HTIR-TC ATR Test*

For the HTIR-TC ATR test, determine the total drift (in %) due to neutron fluence and high-temperature operation for 125 EFPDs by adding the % change due to neutron fluence described in Step 8

of 4.6.1.1 and the % change due to high-temperature operation described in Step 2 of 4.6.1.2.

4.6.2 Results of HTIR-TC Drift Model Calculations

This section provides the results of the Drift Model calculation steps described in Section 4.6.1.

4.6.2.1 *Results for Drift Due to Neutron Fluence*

The following steps are taken to determine the drift caused by neutron fluence:

Determine Temperature Profiles

Temperature profiles were calculated [13] at various times for various HTIR-TCs. Typical results for HTIR-TCs in Capsules 3 and 1 are shown in Figure 12 and Figure 13. Figure 12 shows a temperature

Figure 12. In-reactor temperature profile for HTIR-TC 3-14 in Capsule 3.

profile for HTIR-TC 3-14 in Capsule 3, and Figure 13 shows a temperature profile for HTIR-TC 1-14 in Capsule 1. The profiles encompass several times during the HTIR-TCs' residence in the ATR [10].

The data show a variation of approximately ±5% in calculated temperature for each of the HTIR-TCs at various times in the ATR. However, for the drift calculation, the temperature profile is assumed to remain constant and treat the variation in temperature profiles as a source of noise in the observed drift data for these TCs. For the drift calculation, one HTIR-TC was chosen from Capsule 1 (HTIR-TC 1-14) and one from Capsule 3 (HTIR-TC 3-5), which read the highest temperature of ~1500°C.

Determine Effective Seebeck Coefficient (Unirradiated)

The unirradiated effective Seebeck coefficient was determined for all temperatures in the measurement range by determining the dV/dT vs. temperature from the calibration data for each TC: S(T, Unirradiated) = polynomial fit dV/dT as function of temperature, based on the HTIR-TC calibration data.

A plot of S(T, unirradiated) vs. T for HTIR-TC 1-14 in Capsule 1 and HTIR-TC 3-5 in Capsule 3 is shown in Figure 14 and Figure 15, respectively. A polynomial was fit to this data to provide an equation for the variation of the Seebeck coefficient with temperature. The equation of the polynomial fit to the data is shown in the equations below.

The effective Mo/Nb Seebeck coefficient (unirradiated) for HTIR-TC 1-14 as a function of temperature was determined to be:

. 7

The effective Mo/Nb Seebeck coefficient (unirradiated) for HTIR-TC 3-5 was determined to be:

. 8

In Equations 7 and 8, the units of S are μV/°C, while T is in °C.

Figure 13. In-reactor temperature profile for HTIR-TC 1-14 in Capsule 1.

Figure 14. Effective Seebeck coefficient (unirradiated) for TC 1-14.

Figure 15. Effective Seebeck coefficient (unirradiated) for TC 3-5.

Determine the TC Unirradiated EMF

Calculate the unirradiated EMF of HTIR-TCs in Capsules 1 and 3 of the test fixture by integrating Equation 1, using the temperature profile values shown in Figure 11 and Figure 12, as well as the S(T,x) values calculated via Equations 7 and 8. Since the integration does not have a closed form solution, a numerical integration is performed in which the incremental EMF is calculated for each incremental temperature change and incremental change in distance before adding the incremental EMFs to give the total unirradiated EMF.

Table 7 shows the results of computing the EMF (unirradiated) using Equations 7 and 8 inside Equation 2.

Table 7. Calculated and calibrated EMFs (unirradiated).

HTIR-TC #	Peak Temperature (^{0}C)	Calculated EMF (Unirradiated) (V)	Calibration EMF (V)	Difference (%)
1-14	1280	17812	17900	-0.49
3-5	1500	19400	19672.5	-1.38

Note that, as expected, the calculated EMF (unirradiated) value is approximately equal (within 1.4%) to the measured EMF value for that temperature in the calibration test.

A plot of the temperature profile and calculated incremental EMFs (unirradiated) generated along the length of the TCs is shown in Figure 16 for HTIR-TC 1-14 and Figure 17 for HTIR-TC 3-5.

Note that the temperature and EMF(unirradiated) profiles closely align, as expected.

Figure 16. Temperature and EMF profile for HTIR-TC 1-14.

Figure 17. Temperature and EMF profile for HTIR-TC 3-5.

Determine thermal neutron and fast neutron flux profiles

Calculate the neutron and fast neutron flux profile across all capsules. Based on the ATR description [9], the maximum thermal neutron flux in the middle of Capsule 3 was first assumed to be 4.5×10^{14} nv, but subsequent calculations [13] showed that the maximum thermal flux was reduced to ~2.8×10^{14} nv to account for the capsule perturbation factor. The thermal neutron flux as a function of distance (in ft from the top of the ATR) across the five capsules was determined to obey the following equation:

9

where x is the distance from the top of the reactor in ft. The fast neutron flux was assumed to be unperturbed by the test fixture and estimated to be half the unperturbed thermal flux. The maximum fast neutron flux was 2.2×10^{14} nv, and the profile of the fast neutron flux was assumed to be similar to the thermal neutron flux profile. The fast neutron flux as a function of distance across the five capsules was determined to obey the following equation:

10

A plot of the thermal and fast neutron flux profile across the five capsules is shown in Figure 18.

Estimate Neutron Radiation Effect on Effective Seebeck Coefficient

Calculate the effective Seebeck coefficient reduction due to thermal and fast neutron irradiation. The HTIR-TC Drift Model assumes that the Seebeck coefficient reduction is expressed in form similar to the exponential transmutation equation. Utilizing Equations 3 and 4, the coefficients for drift due to neutron bombardment is as follows:

and

Figure 18. Approximate thermal and fast neutron flux profiles as seen in the capsules of the AGR 5/6/7 test.

where S is the Seebeck coefficient, S^* is the irradiated Seebeck coefficient, $nv_{Thermal}$ is the thermal neutron flux (nv), $nvt_{Thermal}$ is the thermal neutron fluence (nvt), nv_{Fast} is the fast neutron flux (nv), nvt_{Fast} is the fast neutron fluence (nvt), t is the irradiation time (seconds), C_1 is the constant for calculating reduction due to thermal neutrons, C_2 is the constant for calculating reduction due to fast neutrons. Further, the constants are consequently:

1. For C_1, a constant in units of barns (where 1 barn = 10^{-24} cm^2) that considers the transmutations of both HTIR-TCs (Mo and Nb) caused primarily by thermal neutron absorption in the ATR. C_1 is derived from the 2200 m/sec cross section, and, as described in 4.6.1.1, the 2200 m/sec thermal neutron absorption cross section assumed for the Mo/Nb HTIR-TCs is 3.63 barns. The 2200 m/sec cross section, σ, corresponds to an average neutron temperature of T = 20.6°C, and this can be extrapolated, using the following equation, to the cross section, , for the ATR's average thermal neutron temperature of T^* = 60°C [14]:

   11

   where T^* is the new desired temperature and T is 20.6°C—the temperature assumed for all 2200 m/s neutron velocities.

Using Equation 11 to account for the temperature difference between the listed 20.6°C for the 2200 m/sec cross section and 60°C for ATR thermal neutrons, the average effective thermal neutron absorption cross section for Mo in the ATR becomes ~3.02 barns (where 1 barn = 10^{-24} cm^2). The corresponding conservative thermal neutron cross section for estimating drift in a BWR, where the coolant temperature is 550°F (~ 287.8°C), is 2.33 barns. For a PWR, where the coolant temperature is 315°C, it is 2.27 barns.

$$C_1(ATR) = 3.02 \text{ barns} \quad (12)$$

$$C_1(BWR) = 2.33 \text{ barns} \quad (13)$$

$$C_1(PWR) = 2.27 \text{ barns} \quad (14)$$

2. For C_2, experimentally determined constant that accounts for Seebeck coefficient changes due to fast neutron bombardment. The main effect of fast neutron bombardment is the potential change in lattice structure, but there are also some transmutations due to fast and epithermal neutrons. The change in Seebeck coefficient due to fast neutrons takes the same form as that due to thermal neutrons, so the units of constant C_2 are also barns. Though the value of C_2 for fast neutrons is undetermined, it is known to be much less than C_1 for thermal neutrons and is estimated by the Drift Model to be 0.5 barns.

$$C_2(ATR) = 0.5 \text{ barns} \quad (15)$$

$$C_2(BWR) = \text{negligible} \quad (16)$$

C_2(PWR) = negligible 17

Determine Seebeck Coefficient Reduction Factor for Neutron Fluence Corresponding to Specified Full-Power Days in ATR

Calculate the effective Seebeck coefficient reduction factor for a specific length of time that the HTIR-TCs are in the ATR—a period over which the drift can be determined from the data. An evaluation of the data showed that a suitable time was 125 EFPDs. Not all the HTIR-TCs survived this length of time, due to the excessive number of thermal cycles to which the HTIR-TCs were subjected. This life-limiting feature will be discussed in Section 4.7.

Determine the TC Irradiated EMF

Calculate the irradiated EMF of the Capsule 1 and 3 HTIR-TCs in the test fixture by performing a numerical integration of the incremental EMF values for the irradiated TCs. As described in Step 7 of Section 4.6.1.1, the incremental EMFs for the irradiated TCs are calculated by multiplying the incremental temperature change for each incremental distance along the TC by the reduced effective Seebeck coefficient at that location and temperature. The incremental EMFs are then added to give the total irradiated TC EMF.

Using Equations 3–5, the results of computing the EMF(irradiated) of HTIR-TCs 1-14 and 3-5 for the thermal and fast neutron fluence of 125 EFPDs in the ATR test fixture is shown in Table 8.

Table 8. Calculation of EMF (irradiated).

HTIR-TC #	Calculated EMF (irradiated) [V]
1-14	17735
3-5	19289

Calculate HTIR-TC Drift Due to Neutron Fluence

The Drift Model uses Equation 6 to determine the amount of drift.

From the calculations described in Steps 3 and 7 of Section 4.6.2.1, and using the suggested 2200 m/sec Seebeck coefficient reduction constants C_1 and C_2 in Equations 12 and 15 for thermal and fast neutrons, a computation of the drift due to thermal and fast neutron fluence for HTIR-TC 1-14 and 3-5 generated the results shown in Table 9.

Table 9. Drift due to neutron fluence, as calculated by the HTIR-TC Drift Model

HTIR-TC #	Calculated EMF (unirradiated) V]	Irradiation Time (EFPD)	Calculated EMF (irradiated) V]	Calculated Drift [%]
1-14	17812	125	17735	-0.43
3-5	19400	125	19289	-0.57

Since the temperature and flux profiles for HTIR-TC 1-12 and 1-13 are very similar to that for 1-14, the calculated drift for 1-12 and 1-13 is also expected to be -0.43%, the same as for 1-14. Note that this is the calculated drift due only to thermal and fast neutron fluence, and does not include the drift due to prolonged high-temperature operation, which is calculated in Section 4.6.2.2.

4.6.2.2 *Results for Drift Due to High-Temperature Operation*

The below steps are followed to determine the drift due to high-temperature operation.

Determine High-Temperature Drift Data

Data were collected on the drifting of HTIR-TCs heat treated to 1500°C and then placed in a furnace at the high temperature of ~1200°C for >4000 hours [11]. These data, along with a smoothed curve fit to

the data, are shown in Figure 19.

The equation of the 6th order polynomial that smoothly fits the temperature (T) and time (t) data is:

18

Figure 19. Experimental data from HTIR-TC high-temperature drift [11].

Determine High-Temperature Drift in the ATR HTIR-TC Qualification Test

As described in Section 4.6.1.2, the temperature drift data in Figure 19 was converted to relative drift as a function of time. These drift data, which are based on a heat treatment temperature (T_0) and operating temperature (T) of 1500 - 1200 = 300°C, were then extrapolated to the case in which the T - T_0 temperature difference was 1293 - 1450 = -157°C for HTIR-TCs 1-12 and 1-13, 1381 - 1450 = -69 for HTIR-TC 1-14, and 1500 - 1450 = +50°C for HTIR-TC 3-5. The extrapolation was done to preserve the general shape of the high-temperature drift curve and to ensure that, in adding this extrapolated high-temperature drift at 3000 hours to the neutron fluence drift at 3000 hours, the result approximately matches the observed 3000 hour (125 EFPDs) ATR test drift of -3.3% for HTIR-TC 1-12 and 1-13, -3.5% for HTIR-TC 1-14, and -8.7% for HTIR-TC 3-5. The results of the extrapolated drift curves are shown in Figure 20.

The results indicate a relatively small drift when operating at temperatures below the heat treatment temperature, but this drift increases sharply when operating at temperatures higher than the heat treatment temperature. This figure also shows that, if the operating temperature is more than 400°C lower than the heat treatment temperature (i.e., T - T_0 < - 400°C), the drift due to high-temperature operation would become negligeable. The data also show that, if the TC is operating at a temperature higher than the heat treatment temperature (i.e., T - T_0 > +50°C), the magnitude of the drift due to high-temperature operation can exceed 10% for an exposure greater than 3200 hours.

Note that, if these HTIR-TCs were heat treated to temperatures around 1600°C instead of 1450°C, the drift due to high-temperature operation would be much lower. This higher temperature heat treatment of 1600°C is planned for future the construction of HTIR-TCs.

Table 10 shows the results of computing the drift of HTIR-TCs 1-14 and 3-5 caused by high-temperature operation for 125 EFPDs (3000 hours) in the ATR test.

Figure 20. Extrapolated drift (normalized) due to high-temperature operation.

4.6.2.3 *Results for Total HTIR-TC Drift in the ATR Qualification Test*

For the HTIR-TC ATR test, the total drift in % (as calculated by the Drift Model) due to neutron fluence and high-temperature operation for 125 EFPDs was obtained by adding the % change due to neutron fluence and the % change due to high-temperature operation. The results of this calculation are shown in Table 11.

Table 10. Calculation of HTIR-TC drift due to high-temperature operation.

HTIR-TC #	Heat Treatment Temperature [°C]	Operating Temperature [°C]	Time at High Temperature (EFPD)	Drift [%]
1-12	1450	1293	125	-2.86
1-13	1450	1293	125	-2.86
1-14	1450	1381	125	-3.07
3-5	1450	1500	125	-8.08

Table 11. Total calculated HTIR-TC drift due to neutron fluence and high-temperature operation.

HTIR-TC #	Operating Temperature [°C]	Time in ATR (EFPD)	Calculated Drift Due to Neutron Fluence [%]	Calculated Drift Due to High-Temperature Operation [%]	Total Calculated Drift [%]
1-12	1293	125	-0.43	-2.86	-3.29
1-13	1293	125	-0.43	-2.86	-3.29
1-14	1280	125	-0.43	-3.07	-3.50
3-5	1500	125	-0.57	-8.08	-8.65

A comparison of these results (calculated by the HTIR-TC Drift Model) with the observed drift can be seen by examining the drift data obtained for HTIR-TCs 1-14 and 3-5 in the ATR qualification test, in which the drift was due to both neutron fluence and high-temperature operation. The test data for these two HTIR-TCs are shown in Figure 21 and Figure 22.

The data show that, for 125 EFPDs, the total drift due to neutron fluence and high-temperature operation was approximately -3.3% for HTIR-TCs 1-12 and 1-13, 3.5% for HTIR-TC 1-14, and -8.7% for HTIR-TC 3-5. Note that there was no apparent drift for HTIR-TC 3-5 measuring ~1500°C, meaning that HTIR-TCs can be used to measure such high temperatures, without experiencing drift, for 1200 hours. These values compare well with the calculated values shown in Table 10, and the comparison is summarized in Table 12.

4.6.3 HTIR-TC Drift in Operating Thermal BWRs or PWRs

HTIR-TC drift in commercial, well-moderated thermal power reactors can be conservatively estimated by employing the Drift Model and the same 2200 m/sec thermal neutron cross section for determining the Seebeck coefficient reduction factor as was used for the HTIR-TC drift calculation in the ATR. As described in Step 5 of Section 4.6.2, the average cross section for determining the reduction factor in a reactor is obtained by modifying the 2200 m/sec cross section, using Equation 9 to account for the power reactor's thermal neutron temperature. The cross section (C_1) for calculating drift due to neutrons thermalized at ATR, BWR, and PWR temperatures is shown in Equations 10, 11, and 12. Since commercial BWRs and PWRs are primarily thermal flux reactors, the drift due to fast neutron irradiation can be neglected.

Figure 21. Drift data for HTIR-TC 1-14.

Figure 22. Drift data for HTIR-TC 3-5.

The expected thermal neutron fluence (nvt or φt) for a TC located in-core during an 18-month refueling cycle in a commercial power reactor is approximately 3.8×10^{21} nvt and ~5.1×10^{21} nvt for 24 months, based on the average thermal neutron flux over this interval: 8×10^{13} nv. The expected TC drift for this exposure in a BWR or PWR can be calculated by assuming the TC is installed as a standalone TC, and that the neutron flux

Table 12. Comparison of calculated and observed HTIR-TC drift in the ATR test.

HTIR-TC #	Time at High Temperature (EFPD)	Operating Temperature [°C]	Calculated Drift by HTIR-TC	Observed Drift of HTIR-TC in ATR Test [%]	Difference between Calculated and

			Drift Model [%]		Observed Drift [%]
1-12	125	1293	-3.29	-3.33	~ -0.03
1-13	125	1293	-3.29	-3.33	~ -0.03
1-14	125	1381	-3.50	-3.48	~ -0.02
3-5	125	1500	-8.65	-8.67	~ -0.02

incident on the TC is constant in the region where the temperature is changing. For such an installation in a BWR or PWR, the drift can be calculated using the following simple equation:

19

where $C_1(BWR) = 2.33 \times 10^{-24}$ cm^2, $C_1(PWR) = 2.27 \times 10^{-24}$ cm^2. The results of this calculation are shown in Table 13. Another option to consider is the removal of Niobium neutron absorption cross section as a negligible amount of EMF is generated in that thermoelement. Molybdenum would then be considered the only generator of EMF and leaves the neutron absorption cross section of the HTIR-TC as 2.48 barns.

Table 13. Calculated drift in a commercial power reactor.

Power Plant	Total Cross Section [barns]	Refueling Cycle [months]	Average Thermal Flux [nv]	Thermal Neutron Fluence [nvt]	C_1 [cm^2]	Drift [%]
BWR	3.63	18	8×10^{13}	3.79×10^{21}	2.33×10^{-24}	-0.86
BWR		24		5.05×10^{21}	2.33×10^{-24}	-1.17
PWR		18		3.79×10^{21}	2.27×10^{-24}	-0.88
PWR		24		5.05×10^{21}	2.27×10^{-24}	-1.14
BWR	2.48*	18		3.79×10^{21}	2.33×10^{-24}	-0.60
BWR		24		5.05×10^{21}	2.33×10^{-24}	-0.80
PWR		18		3.79×10^{21}	2.27×10^{-24}	-0.59
PWR		24		5.05×10^{21}	2.27×10^{-24}	-0.78

*Niobium neutron cross section removed from total cross section as minimal EMF is contributed.

Note that, for HTIR-TCs operating in a BWR or PWR, the only drift is due to neutron exposure. The drift due to high-temperature operation in a BWR or PWR is negligible, since the operating temperature is much smaller than the heat treatment temperature. The typical operating reactor temperature at 100% power is 300°C for a BWR and 315°C for a PWR, while the heat treatment temperature for these HTIR-TCs is 1450°C. Thus, for normal full-power operation, the difference between the heat treatment temperature and the operating temperature (>1100°C) is very large and would produce a negligible high-temperature drift. Also note that even if the TC was measuring a BWR/PWR accident temperature of 1000°C, the difference with the heat treatment temperature would be >400°C. Therefore, according to the Drift Model, the high-temperature drift would be negligible, especially since the accident time is generally short. However, it is important even with these low temperature considerations, it is imperative that the TC be properly heat treated over the length of cable that will be immersed in any temperature gradient in the reactor core. This assures a uniform wire and that bias error in the calibration of the TC is insignificant when different temperature gradients are being measured.

In a BWR/PWR, the calculated drift is < 1% for a thermal neutron fluence of ~3.8×10^{21} nvt, which meets the requirement in the F&OR report and is considered acceptably small to justify installation in a BWR or PWR for one or possibly two 18-month refueling cycles. Note that the drift estimate of 1% is conservatively high for BWRs/PWRs, since the cross section used in the calculation is higher than

expected. Further, using the reasoning from Table 13, it is estimated that the HTIR-TC could survive for up to 24 months inside advanced reactors and/or Gen III+ reactors.

Since the TCs in a BWR or PWR will be measuring a much lower temperature than in the ATR qualification test, this will decrease the drift due to any heat treatment deficiencies created during TC manufacture. Note that the cross section used for determining the drift in BWR or PWR is based on the drift data of the HTIR-TC in the ATR qualification test and provides an appropriate and justifiable basis for the drift model estimate in a BWR or PWR at these lower temperatures. As discussed in the F&OR report, the 18-month duration in a BWR or PWR is also considered the life of the TC, based on drift without recalibration. Note that the thermal neutron fluence corresponding to this EOL has been changed to the more realistic specified value of 3.8×10^{21} nvt, and this change has been applied in both the revised F&OR report and the revised Qualification Requirements report.

4.7 HTIR-TC Life

There are basically two reasons why HTIR-TCs will reach EOL:

1. Drift greater than that which can be tolerated for accurate measurements without TC recalibration
2. Thermal transients that can cause a mechanical break in the TCs.

HTIR-TC performance in these categories is described below.

4.7.1 End-of-Life Due to Excessive Drift

HTIR-TC performance in the drift category has already been described in Section 4.6. Included in this description is the drift due to neutron fluence (thermal and fast), the drift due to prolonged operation at high temperature, and HTIR-TC drift performance in the ATR qualification test and for potential operation in a commercial power reactor (i.e., BWR or PWR). HTIR-TC drift of <3.5% resulted from 125 EFPDs in the ATR when operated at 70°C below the heat treatment temperature of 1450°C. The test results were extrapolated to show that the drift for 18 months of operation in a BWR/PWR would be <1%, since the operating temperature is low enough that no drift occurs due to high-temperature operation. Note that, as stated in Section 4.5, the change in the specified TC EOL to reflect these values based on data from the HTIR-TC qualification test was applied in the revised F&OR report and revised Qualification Requirements report.

4.7.2 End-of-Life Due to Mechanical Failure

The HTIR-TC's mechanical EOL is a measure of how long the EMF output is produced before the TC electrical connection breaks and the output drops to zero. The HTIR-TC is built to be rugged while in situ within the reactor core, and consideration has been given to (1) forming the junction using a mechanical swage instead of a weld, (2) flexibility in order to withstand the installation, and (3) the ability to withstand several drastic thermal transients expected during normal and abnormal reactor operation. However, catastrophic failure (i.e., EOL) is expected for all high-temperature, high-neutron-flux TCs as a result of a breakage in the electrical connection due to embrittlement and thermal strain resulting from the high-temperature nuclear environment. The lifetime thermal fluence is generally used as a measure of how long an HTIR-TC is operational, though thermal fluence is not the cause of the catastrophic failure. No numerical values exist for the conditions leading to catastrophic failure, though it is hoped that catastrophic failure would occur after the TC has reached its EOL due to drift.

Table 14 shows the measured operating life of the HTIR-TCs in Capsules 1 and 3, based on the performance data shown in Figure 3 and Figure 5, and in Table 3.

For comparison purposes, Table 15 shows the measured operating life of the other type N TCs in the AGR 5/6/7 capsules. In comparing these results to those in Table 13, it is clear that, besides being able to measure higher temperatures, the HTIR-TCs generally lasted longer than the other type N TCs.

A major cause of catastrophic failure EOL is electrical connection breakage due to thermal stress and the strain from thermal expansion at high temperatures, as well as from rapid thermal transients such as

those which could occur from multiple fast reactor shutdowns and startups.

A requirement that the HTIR-TCs be able to withstand the thermal transients caused by five startups and five shutdowns in a test reactor such as the ATR was stated in the F&OR report and the Qualification Requirements report, and it is expected that, for typical power reactors in which the reactor temperature change rate is greatly reduced (typically 100°F/hr [38°C/hr] in a BWR), catastrophic failure from this

Table 14. Measured HTIR-TC life in the AGR 5/6/7 test.

Capsule #	HTIR-TC #	Approximate Measured Temperature [°C]	Measured Life in AGR 5/6/7 Test (EFPD)
1	1-12	1279	120
1	1-13	1272	87
1	1-14	1337	161
1	1-15	1390	120
3	3-5	1453	125
3	3-12	1279	166
3	3-14	1200	164

Table 15. Measured life of other type N TCs in the AGR 5/6/7 test.

Capsule	Thermocouple	Measured Temperature [°C]	Measured Life in AGR 5/6/7 Test [EFPD]
1	Type N 1-4	956	112
1	Type N 1-6	971	43
1	Type N 1-7	943	57
1	Type N 1-8	950	111
3	Type N 3-7	1163	46
3	Type N 3-13	1154	243
3	Type N 3-15	1156	125

cause will occur far less often. A third cause of catastrophic failure is the chance of electrical connection breakage due to stress and strain from thermal expansion/contraction after embrittlement due to neutron irradiation. It is hoped that the HTIR-TCs can tolerate the thermal expansion stress for the desired life of 125 EFPDs in the ATR. However, the data showed that four HTIR-TCs met this criterion, while four did not. The reason for not meeting the 125 EFPD requirement was due to the abnormally large number of severe thermal transients that the HTIR-TCs endured. It is likely that all would have met the criteria of 3% drift over 125 EFPDs had they only encountered the specified number of five startup and five shutdown thermal transients.

4.7.3 TC Life vs. Thermal Transients

An examination of the data showed that all the TCs failed (i.e., no output) during either a reactor startup or shutdown transient. This indicates that thermal transients, especially severe ones such as during ATR startup/shutdown, are an important parameter in determining the EOL of TCs. The TCs, as part of the AGR-5/6/7 test fixture, underwent several severe thermal shock transients when the reactor was rapidly shut down and restarted several times during its residence in the reactor, and these TCs failed after multiple such transients.

The data in Figure 3 and Figure 5 show that, over a 150 calendar day period, the reactor was rapidly shut down and restarted five times, corresponding to the production of 10 such thermal transients—the specified life of the HTIR-TC with respect to surviving rapid thermal transients, as specified in the F&OR report [1]. The data showed that all the HTIR-TCs survived these transients; therefore, they all met this

EOL requirement. Note, however, that these thermal transients occurred more often than expected; and for some, the corresponding exposure was less than the 125 EFPD requirement and occurred prior to a 3% drift being measured. The data showed that most HTIR-TCs survived double the specified number of severe 100%-power-to-shutdown and shutdown-to-100%-power thermal transients, demonstrating that

Table 16. HTIR-TC EOL vs. ATR startup/shutdown thermal transients.

HTIR-TC	Number of Transients for EOL	Calendar Days	EFPD [Days]
1-12	19	380	120
1-13	14	188	87
1-14	16	387	161
1-15	14	430	120
3-5	21	383	125
3-12	22	430	166
3-14	21	421	164

the HTIR-TC mechanical design is likely rugged enough to more than meet the specified requirement of withstanding 10 thermal shock transients. A summary of HTIR-TC EOL vs. the number of startup/shutdown data is shown in Table 16.

5. SUMMARY OF HTIR-TC PERFORMANCE IN QUALIFICATION TEST

A summary of the results from the HTIR-TC qualification test measurement and requirements are shown in Table 17, Table 18, and Table 19 for the HTIR-TC calibrations, AGR 5/6/7 Capsules 1 results, and AGR 5/6/7 Capsule 3 results, respectively.

Table 17. The general repeatability and accuracy from the calibration test for all HTIR-TCs.

Parameter	Requirement	Value in Calibration
Repeatability	±1%	< 0.3%
Accuracy	±1%	0.4% above 100°C 1°C below 100°C

Table 18. Summary of HTIR-TC performance in the Capsule 1 qualification test.

Parameter	Requirement	Measured Value of HTIR-TCs in Capsule 1			
		1-12	1-13	1-14	1-15
Temp Range Min [°C] Max [°C]	Room Temp 1550°C	21.31 1354	22.96 1350	21.45 1412	21.20 1259
Accuracy [%]	±1%	Test not designed to measure TC accuracy to within 1%. HTIR-TC temperatures agreed to within 5% of the theoretically calculated temperatures, which is within the accuracy of the theoretical calculations.			
Repeatability [%]	±1%	±1%	±1%	±1%	±1%
Drift in ATR due to neutron fluence (calculated)	-3.5 % (For 125 EFPDs)	-0.43% (calc)	-0.43% (calc)	-0.43% (calc)	--

Parameter	Requirement	Measured Value of HTIR-TCs in Capsule 1			
		1-12	1-13	1-14	1-15
Drift in ATR due to high temperature (calculated)		-2.9%	-2.9%	-3.1%	--
Total drift in ATR (calculated)		-3.3% (calc)	-3.3% (calc)	-3.5% (calc)	--
Total drift in ATR [%] (measured)	-3.5 % (for 125 EFPDs of exposure at ATR when operating at less than the heat treatment temperature)	-3.3% at 125 EFPDs (Note: The drift value at 125 EFPD is extrapolated, since the TC only survived to 120 EFPDs)	-3.3% at 125 EFPDs (Note: The drift value at 125 EFPD is extrapolated, since the TC only survived to 87 EFPDs)	-3.5% at 125 EFPDs	Not measurable due to noise in the data
Drift in BWR [%]	<1%	-0.86% (calculated)			
Drift in PWR [%]	<1%	-0.86% (calculated)			
End-of-Life					
Exposure (EFPD)	125	120	87	161	120
Thermal transients Reactor startups Reactor shutdowns	 5 5	 10 9	 7 7	 8 8	 7 7

Table 19. Summary of HTIR-TC performance in the Capsule 3 qualification test.

Parameter	Requirement	Measured Value of HTIR-TCs in Capsule 3		
		3-5	3-12	3-14
Temp Range Min [°C] Max [°C]	 Room Temp 1550°C	 23.12 1515	 22.97 1552	 22.70 1353
Accuracy (%)	±1%	Test not designed to measure TC accuracy to within 1%. HTIR-TC temperatures agreed to within 5% of the theoretically calculated temperatures, which is within the accuracy of the theoretical calculations.		
Repeatability (%)	±1%	±1%	±1%	±1%
Drift in ATR due to neutron fluence (calc)	-3.5 % (For 125 EFPDs)	-0.57%	--	--
Drift in ATR due to high temperature (calc)		-8.1%	--	--
Total drift in ATR (calc)		-8.7%	--	--
Total drift in ATR (%) (measured)	-3.5 % (For 125 EFPDs of exposure at ATR when operating at less than the heat treatment temperature)	-8.7% at 125 EFPDs (due mainly to prolonged operation at a temperature 50°C higher than the heat treatment temperature)	Virtually no measurable drift at up to 125 EFPDs, but likely -3% or -4% drift, which was undetected since the temp was controlled by a TC whose sensitivity was decreasing.	Drift not measurable due to an increase in ambient temperature. Would likely meet the drift req't of -3% or -4% if ambient temp was constant.
Drift in BWR (%)	<1%	0.86% (calculated)		
Drift in PWR (%)	<1%	0.88% (calculated)		
End-of-Life				
Exposure (EFPD)	125	125	166	164
Thermal transients Reactor startups Reactor shutdowns	 5 5	 11 10	 11 11	 11 10

Results of the qualification test show that the HTIR-TCs met most of the requirements specified in the F&OR report and the Qualifications Report.

1. **Range**: The TCs were able to accurately measure temperatures ranging from room temperature to 1515°C. This fell short of the requirement of 1600°C, due to the test fixture not being designed to measure at a higher temperature. This was the highest temperature measured by any TC in a high-flux reactor environment. Note that type N TCs, which are typically used for high-temperature measurements, can only measure up to approximately 1300°C, due to melting point restrictions—almost 300°C less than the HTIR-TCs.
2. **Accuracy**: The HTIR-TC accuracy was determined in the out-of-pile calibration test where the HTIR-TC temperature measurement was compared to the temperature measurement by the NIST standard. The accuracy was not determined in the ATR test since the test fixture was not designed to measure HTIR-TC accuracy to within the stated 1%, and did not include a reliable standard for measuring the ambient temperature to within 1% in high temperature range. In fact, the HTIR-TCs were used to validate the theoretical calculations. It is estimated that the theoretical calculations of the ambient temperature were only accurate to within approximately 5%, and all the HTIR-TC measurements fell within 5% of the theoretically calculated ambient temperatures.
3. **Repeatability**: The repeatability of all TCs was tested by comparing the pre- and post-shutdown values. It was determined that the measurements were repeatable to within the specified accuracy value of ±1%.
4. **Drift**: This performance feature was unable to be determined accurately because of the noise in the data due to variations in ambient temperature, and because the TCs endured far more than the five specified severe full-power/shutdown thermal transients. The four HTIR-TCs in Capsule 1 behaved as expected from a drift point of view. The HTIR-TCs in Capsule 1 (1-12, 1-13, and 1-14) had a drift that met the -3.5% requirement at 125 EFPDs, though some failed before reaching 125 EFPDs, having been subjected to a large (more than the specified) number of severe thermal transients. The three HTIR-TCs in Capsule 3 reflected different drift performance trends. HTIR-TC 3-14 showed an upward trend that was synchronous with four other type N TCs—a trend attributed to a gradual increase in ambient temperature, due to changes in the gas cooling system, and also because the temperature was controlled by a control TC that was decreasing in sensitivity. The performance data indicate that this TC would have behaved as expected had this increase in ambient temperature not occurred. HTIR-TC 3-12, along with two other type N TCs, behaved normally and showed virtually no drift, but held constant. HTIR-TC 3-5 behaved as expected at an exposure of 150 EFPDs. The performance data indicate that this TC would have actually shown a drift of -3 to -4% at an exposure of 125 EFPDs if the ambient temperature failed to reach a neutron fluence exposure of 50 EFPDs, but then showed a large drop of ~8.7 % at 125 EFPDs. The cause of this large sensitivity decrease is due to prolonged operation at a high temperature that exceeded the heat treatment temperature by 50°C. The technical reason for this is not well understood but is likely due to changes in the TC metallurgical grain structure and the possible diffusion of impurities into the thermoelements, due to prolonged operation at high temperatures. Note that the drift measurements were made at high ATR power, and the HTIR-TC drift values calculated by the drift model described in this report apply only to high temperature operation (> 1050 deg C). No HTIR-TC drift measurements were made at low ATR power and no experimental results are available for low temperature operation.

A HTIR-TC Drift Model was developed to calculate TC drift. It was determined that, based on the experimental data, that HTIR-TC drift was due to a reduction of the thermoelements' Seebeck coefficients by both thermal and fast neutrons, and also by prolonged operation at high temperature. The thermal neutrons change the Seebeck coefficient by transmuting the thermoelements via absorbing thermal neutrons, and the fast neutrons change the Seebeck coefficient primarily by altering the thermoelements' lattice structure through fast neutron bombardment. In addition, prolonged operation at high temperature can change the metallurgical structure of the thermoelements and cause drift. Constants

for these effects were determined from the available experimental data and used, along with estimates of the temperature and neutron flux profiles across the TC cables, to determine the TC EMFs pre- and post-irradiation and calculate the TC drift due to neutron fluence and prolonged operation at high temperature. The calculation showed that, for 125 EFPDs of exposure in the ATR test fixture, the drift was ~3.3 % for HTIR-TCs 1-12 and 1-13, 3.7% for HTIR-TC 1-14 in Capsule 1, and ~8.7% for HTIR-TC 3-5 at a higher temperature in Capsule 3. The calculated drift matched the observed drift for HTIR-TCs in Capsule 1, but not in Capsule 3, due to the uncontrolled temperature increase in Capsule 3.

5. **End-of-Life:** The qualification test requirements defined the HTIR-TC EOL as whichever came first: enduring the thermal transients from five startups and five shutdowns (which could break the electrical connection and result in catastrophic failure), or surviving an ATR exposure of 125 EFPDs (ensuring that the TCs could survive at least one 18-month refueling cycle in a commercial, well-moderated thermal power nuclear reactor in which the thermal neutron fluence for an 18-month exposure is 3.8×10^{21} nvt). HTIR-TC EOL was evaluated against both the drift exposure and thermal transient criteria. The results showed that all HTIR-TCs survived more than the specified five startup and five shutdown thermal transients, and all except one would have met the drift criteria had their life not been cut short by encountering too many severe shutdown/startup and startup/shutdown thermal transients. These data indicate that, for a power reactor in which the operating temperatures are quite low (~200°C), and thermal transients are much less severe than those encountered in the ATR test fixture, the HTIR-TCs can survive at least one 18-month refueling cycle in a commercial, well-moderated thermal power nuclear reactor, with a drift of <1%.
6. **Response Time:** This performance parameter was not measured in the test. However, based on a comparison of the HTIR-TC design (1/16 in. OD) with other established similar-sized TC designs with response times of approximately 0.2 seconds, it is clear that the HTIR-TC will meet the conservatively specified requirement of 0.5 seconds.

6. CONCLUSIONS

The following conclusions have been made from this report:

- Based on the results of the HTIR-TC qualification test, in which the TCs were part of the AGR 5/6/7 experimental test fixture in the ATR, the present HTIR-TC design should be considered a qualified TC for the following applications:
  - Standalone TC in a commercial, well-moderated power reactor for measuring reactor temperatures of <1050°C for a full 18-month refueling interval, as long as the temperature change during normal startup or shutdown is controlled and kept below ~50°C/hour. The drift for this application using the conservative HTIR-TC neutron absorption coefficient of ~2.3 barns is expected to be <0.9%. If the refueling interval was increased to 24 months, the drift would increase to ~1.2%. Note that by not considering the absorption coefficient of Niobium (since the Niobium does not contribute significantly to the EMF) the HTIR-TC neutron absorption cross section decreases to a potentially more realistic value of 1.59 barns, the HTIR-TC drift decreases to < 0.6% for 18 month and 0.8% for 24 month refueling cycles. It is likely that HTIR-TC is really designed to measure high temperatures it will not be used as the main but as a back-up instrument for measuring the normal low commercial power reactor inlet and outlet temperatures, and mainly be used to measure the high temperatures that could result if there was a loss of coolant accident.

    Note that the 1050°C value is >650°C higher than the core outlet temperature for these reactors, and well below the heat treatment temperature of the HTIR-TCs. In this application, the HTIR-TC can, in the event of an accident, also be used to measure core temperatures of up to ~1500°C for a short period (i.e., approximately 1200 hours) before the reactor is shut down and the temperature cools, without entailing any drift concerns during the presumably short duration of this high-temperature transient. There have already been several inquires from NPPs for use of HTIR-TCs.

- Standalone TC in any commercial, non-nuclear facility for measuring temperatures of <1050°C over a prolonged period. The drift for this application should be <0.5%, since no drift is caused by neutron fluence effects. Accurate measurements should also be possible at up to 1500°C, at least for a short time (i.e., approximately 1200 hours) during a high-temperature transient. For this application also, the temperature change during normal startup or shutdown should be kept below ~50°C/hour.
- TC in a test fixture for conducting fuel experiment tests in a test reactor such as the ATR. For such applications, if the temperature is controlled to within 1%, temperature measurements of up to 1500°C are feasible over a period of 125 EFPDs, with a drift of <4% when the peak thermal flux is ~2.8×10^{14} nv and the fast flux is ~2.3×10^{14} nv. Also, provisions should be made for accurate temperature and neutron flux profile calculations and/or measurements along the length of the TC cable. For this application, the severe thermal transients due to fast startup/shutdown should be kept below five. The INL has already received requests for the use of HTIR-TCs in other test reactors (MITR).

  Note that, for all three applications, if the TC is heat treated to a maximum temperature of 1600°C (as is planned for the future), higher temperature measurements can be sustained for longer periods of time without drift. Note also that the length of HTIR-TC thermocouple that needs to be heat treated would depend on the application.

  Some additional design improvements can be evaluated in the future, depending upon the application and intended use of the HTIR-TC:

- Heat treating at a higher temperature (1600°C) when it is intended for use in measuring high temperatures (>1500°C) over a long period of time in a high-flux nuclear reactor
- Adding a spring to the TC design so as to lessen the impact of stress and strain due to thermal expansion. Clearly, the present design is well qualified for use in current power reactors, in which the stress and strain due to thermal transients is much less than those encountered in the ATR qualification test. Also, an additional post-irradiation examination test should be considered in order to determine where the breaks in failed HTIR-TCs have occurred. This test can be conducted using a simple, readily available time-domain reflectometer.

7. REFERENCES

1. Skifton, R., "High Temperature Irradiation Resistant Thermocouple Qualification Requirement Report", Idaho National Laboratory, INL/EXT-21-63269, 2021.
2. Palmer, A.J., Petti, D., Grover, S.B., "Advanced gas reactor (AGR)-5/6/7 fuel irradiation experiments in the advanced test reactor," International Congress on Advances in Nuclear Power Plants, ICAPP 2014, Vol. 1. pp. 257-266, 2014.
3. Skifton, R., "High Temperature Irradiation Resistant Thermocouple Preliminary Design Report," INL/INT-20-60511, Idaho National Laboratory, INL/EXT-21-63198, 2021
4. Skifton, R., "High Temperature Irradiation Resistant Thermocouple Preliminary Calibration Report," INL/INT-20-60512, Idaho National Laboratory, INL/EXT-21-63172, 2021
5. Palmer, A.J., "HTIR Thermocouples for AGR-5/6/7," Idaho National Laboratory, SPC-1963, Rev 3, 02/27/2017.
6. Skifton, R., "High Temperature Irradiation Resistant Thermocouple Function and Operation Report," Idaho National Laboratory, INL/EXT-21-63173, 2021.
7. Scates, D., Reber, E.L., Miller, D., "Fission gas monitoring for the AGR-5/6/7 experiment," *Nuclear Engineering and Design*, **358**, 2020. https://doi.org/10.1016/j.nucengdes.2019.110417.
8. T Pham, C.B, Sterbentz, J.W., Hawkes, G.L., Scates, D.M. Palmer, J., "AGR-5/6/7 Experiment Monitoring and Simulation Progress," INL External Report, INL/EXT-19-55429, 2020.

https://www.osti.gov/servlets/purl/1689160.

9. "Advanced Test Reactor National Scientific User Facility Users Guide", Idaho National Laboratory, INL/EXT-08-14709, 2009. https://nsuf.inl.gov/File/ATRUsersGuide.pdf.
10. Palmer, A.J., "HTIR-TC Fabrication Process for AGR 5/6/7," Idaho National Laboratory, TEV-2791, 2017.
11. Rempe, J.L., Knudson, D.L., Condie, K.G., Wilkins, S.C., "Evaluation of Specialized Thermocouples for High-Temperature In-Pile Testing," (INL/CON--05-00944), ICAPP Reno, NV, 2006. https://digital.library.unt.edu/ark:/67531/metadc887562/.
12. Scervini, M., Rae, C., Lindley, B., "Transmutation of thermocouples in thermal and fast nuclear reactors," 2013 3rd International Conference on Advancements in Nuclear Instrumentation, Measurement Methods and their Applications (ANIMMA), Marseille, pp. 1-8, 2013.
13. Hawkes, G.L., "Thermal Model Details and Description of the AGR-5/6/7 Experiment," 2019. https://www.osti.gov/biblio/1599861-thermal-model-details-description-agr-experiment.
14. Wescott, C.H., "Effective Cross Section Values for Well-Moderated Thermal Reactor Spectrum", Atomic Energy of Canada Limited, AECL-1101, 1962. https://inis.iaea.org/search/search.aspx?orig_q=RN:41057250.